https://ntrs.nasa.gov/search.jsp?R=19720005655 2020-03-11T21:50:40+00:00Z

COLLEGE OF FORESTRY AND NATURAL RESOURCES

Department of Watershed Science

COLORADO STATE UNIVERSITY

FORT COLLINS, COLORADO

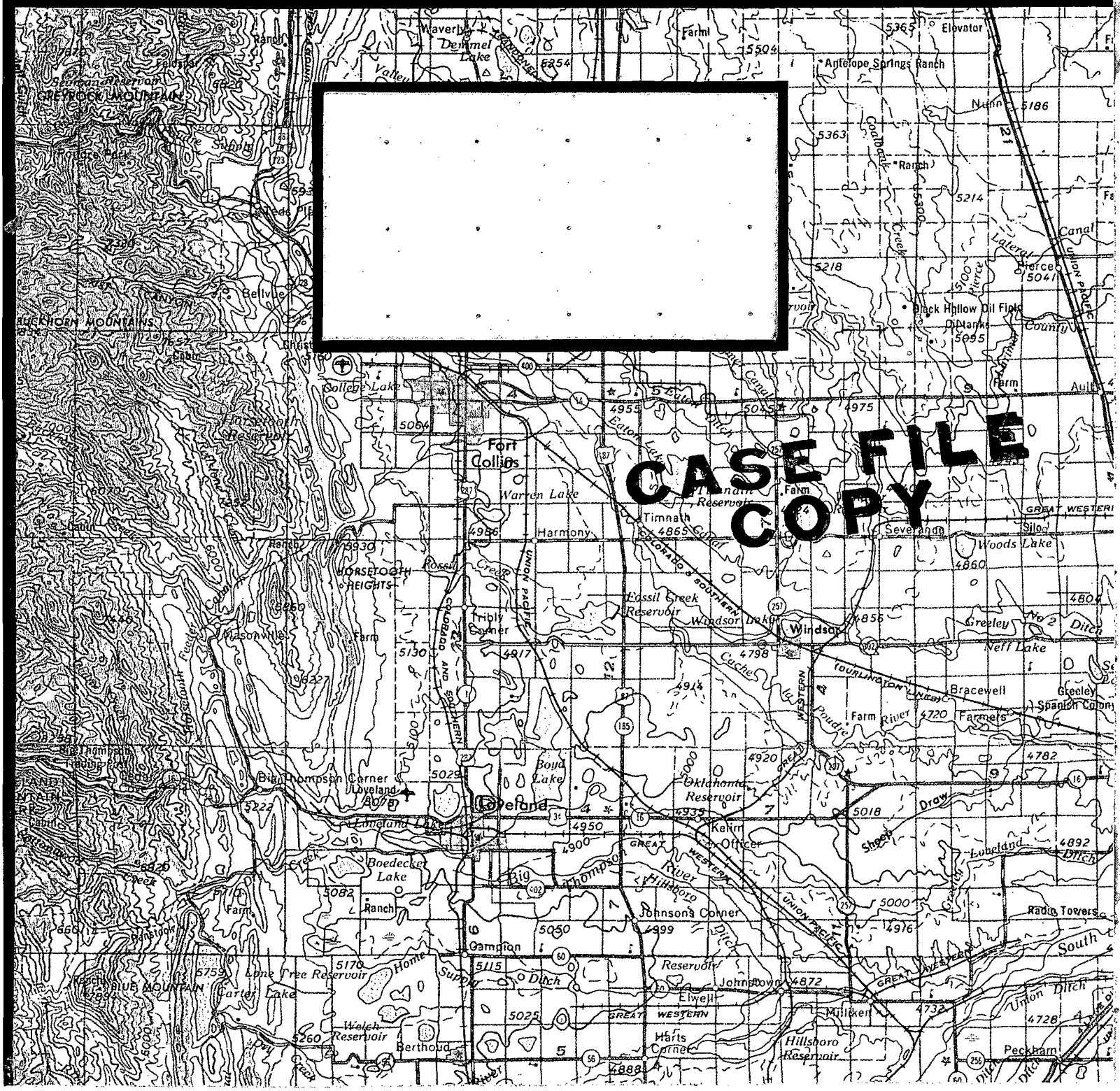

July, 1971

N 72-19304

MATHEMATICAL MODELS FOR RADIATION TRANSFER

W. E. Marlatt
J. C. Harlan
H. L. Cole

Final Report: NGR 06-002-038

"Radiation Transfer"

Department of Watershed Sciences

Colorado State University

Fort Collins, Colorado

TABLE OF CONTENTS

ABSTRACT

This is the final report of project "Radiation Transfer," NASA grant NGR 06-002-038, which is a subproject under the main project entitled "Biology and Engineering of Space and Planetary Life Systems." A radiation transfer model was modified to include semitransparent and opaque layers as well as molecular constituents. An example of the use of the program and an analysis of the mathematical model are included in this report.

ACKNOWLEDGEMENTS

The authors wish to thank the following persons for their contributions to this report: Dr. Stephen Cox, Associate Professor in the Atmospheric Science Department, Colorado State University; Dr. Peter Kuhn, atmospheric scientist at NOAA-ERL; Mrs. Charlene Polifka and Mr. Loren Snyder, systems analysts; Mrs. Julie Hjermstad, data technician; Mr. Donald Hill, research technician; and Mr. Dwain Adam, CSU pilot.

I. INTRODUCTION

This is the final report of project "Radiation Transfer," NASA grant NGR 06-002-038, which is a subproject under a university project entitled, "Biology and Engineering of Space and Planetary Life Systems." The primary objective of the research program was "to investigate the role of semitransparent (haze, cirrus clouds) and opaque (water drop clouds) layers on the transfer of visible and infrared radiation through the atmosphere." During the last year of this grant, the project effort was directed toward the modification of a suitable radiation transfer mathematical model (described in detail later in this report) to allow inclusion of cloud or haze layers in infrared energy transfer calculations. Field programs conducted previously had been concentrated in the wavelength region of the 8 - 12 micron atmospheric window in the thermal infrared. The numerical model of the radiative transfer equation used in this study covers the spectral region from 5 micron to 100 micron, inclusively.

RADIANV, the radiation transfer model, was developed by Drs. S. Cox and P. Kuhn while at the University of Wisconsin. In order to model radiation transfer through turbid atmospheres, Cole, assisted by Dr. Cox, undertook the modification to include semitransparent and opaque aerosol layers in RADIANV.

This report includes an explanation of the physics and mathematical analysis of RADIANV (section II) and of EXTCOEF (section IV) plus a flow chart of each program (sections III and V, respectively). An example of the use of the program is included as Appendix III. The example is a

comparison of calculations by RADIANV for observations of a clear sky case and a cloudy sky case. The radiance data were collected by Kuhn, NOAA, Boulder, aboard the NASA CV990 during the 1967 meteorological flights. The cloud drop data were taken at the same time by Marlatt aboard the Colorado State University aircraft. Appendix I is a sample of the computer printout for each of the three calculation options of RADIANV and a sample of printout from EXTCOEF.

II. PHYSICS AND MATHEMATICAL ANALYSIS

A. Theoretical Calculation of Atmospheric Radiance.

The radiative transfer program calculates the radiance at a reference level from the atmosphere above that level. It is calculated as a function of wavelength over the interval which corresponds to the spectral bandpass of the instrument being simulated. The basic equation for the calculation of the radiance $N\lambda(p,T)$ at wavelength λ, received at a pressure altitude P_o from the atmosphere above that level, may be expressed as

$$(1) \quad N\lambda\,(p,T) = \int_{po}^{p} N\lambda(Tp)\,\frac{dT\lambda}{dp}\,dp$$

where $N\lambda(T)$ is the blackbody radiance at temperature T and Tp is the atmospheric temperature at pressure altitude p. This can be approximated by dividing the atmosphere into a series of isothermal layers and replacing the integral term by a sum of terms representing the contribution of each individual layer:

$$(2) \quad N\lambda(p,T) = \sum_{i} N\lambda(\bar{T}i)\Delta T\lambda i$$

where Ti is the mean temperature of atmospheric layer i; and $\Delta T\lambda i$ is the difference in transmission from the top of layer i to the observation level p_o, and the bottom of layer i to the observation level p_o.

The wavelength interval of interest (i.e. spectral bandpass of the instrument) is changed to a wavenumber interval and then this interval is divided into 10 wavenumber increments. The mean wavenumber is determined for each increment and then these wavenumbers are used in the radiance calculation. The total radiance received at the reference level can be expressed as

$$(3) \quad N_{TOT} = \int_{\nu 1}^{\nu 2}\int_{p_o}^{p} N\nu(T)\,\frac{dT\nu}{dP}\,dP\;\;d\nu$$

As already mentioned the spectral interval ($\nu 1 - \nu 2$) has been divided into ten wavenumber increments; therefore, the intergral over wavenumber can be replaced by a summation. By substituting the summation over layers as shown in equation (2) we can express the equation for total radiance as follows:

$$(4) \quad N_{TOT} = \sum_{\nu 1}^{\nu 2}\sum_{p_o}^{p} N\nu(T)\Delta T\nu\;\Delta\nu$$

where $\Delta\nu$ is equal to 10 wavenumbers.

Calculations may start at any pressure level in the atmosphere. For downflux, the atmosphere is divided into the desired number of layers from the selected reference level up to 50 mb. The remaining layers above 50 mb are divided into the following intervals:

a. 50 mb - 25 mb
b. 25 mb - 10 mb
c. 10 mb - 6 mb
d. 6 mb - 2 mb
e. 2 mb - 1 mb

In the present program 1 mb is essentially considered as the top of the atmosphere. In order to perform the calculation, data for these various levels must be input into the program. The necessary data required at each level are pressure, temperature, water vapor mixing ratio, carbon dioxide mixing ratio , and ozone mixing ratio. Radiosonde data is used to determine temperature, pressure, and water vapor mixing ratio up to the radiosondes maximum level. Climatological data for stratospheric water vapor is used above the radiosonde level and a mean distribution of ozone density is used for the ozone mixing ratio. The carbon dioxide mixing ratio is assumed to be constant in the program, but could be included as a variable mixing ratio if desired.

B. The Calculation of Atmospheric Transmission

1. Atmospheric Gases

Elsasser's method is used to determine the atmospheric transmission for the various gases. This means that the transmissivity of the gas is a function of

$$(5) \quad T = T\ (\log u^* + \log L)$$

where u* is the reduced optical mass and L is the generalized absorption coefficient. To determine the transmissivity, the generalized absorption coefficients are used in the program as a look-up table and modified optical thickness is calculated using the following equation

$$(6) \quad u^* = u\left(\frac{p}{1000}\right)^{\gamma}\left(\frac{273.16}{T}\right)^{.5}$$

The transmission functions are also input into the program as look-up tables and the transmissivity is then determined from the sum of the log u^* + log L.

2. Aerosols

The atmospheric transmissivity for an aerosol layer is determined from the equation

$$(7) \quad T = e^{-BU}$$

where B can be the extinction, absorption, or scattering coefficients and U is the optical depth (KM) of the layer.

The extinction, absorption and scattering coefficients are determined in another program using the following equations:

$$(8)\quad K_{EXT}(x,m) = 2/x^2 \sum_{n=1}^{\infty}(2n+1)\ \mathrm{Re}\{an + bn\}$$

$$(9)\quad K_{SCAT}(x,m) = 2/x^2 \sum_{n=1}^{\infty}(2n+1)\ \{1\ anl^2 + 1\ bnl^2\}$$

$$(10)\quad K_{ABS} = K_{EXT} - K_{SCAT}$$

where

K_{EXT} = Extinction Cross Section

K_{SCAT} = Scattering Cross Section

K_{ABS} = Absorption Cross Section

$x = 2\pi a/\lambda$ - MIE SIZE Parameter

m = Complex Index of Refraction

an & bn = MIE Complex Scattering Coefficients

$$(11)\quad B(m,\lambda;\ x_1x_2) = \pi \int_{x_1}^{x_2} x^2\ f(x,k)\ K(m,x)\ dx$$

where

B = extinction, absorption, or scattering coefficients
K = extinction, absorption, or scattering cross sections
f(x,k) = aerosol size distribution function
x_1 & x_2 = the lower and upper limits in the particle size

B_{EXT}, B_{ABS}, and B_{SCAT} coefficients are determined for each 10 wavenumber increments over the spectral bandpass and for each aerosol distribution function (i.e. continental, maritime). These coefficients are then imput into the radiative transfer program as a look up table.

C. Using the Calculated Transmissivities to Determine the Atmospheric Radiance

The transmissivity functions are used in equation (4) in the ΔT term. ΔT for each layer is determined by the following equation:

$$(12)\quad \Delta T = DT*TEBAR+TTT3$$

where

DT = T2(I)*T2C(I)*T2W(I)*T2)Z(I)-T1(I)*T1C(I)*T1W(I)*T1OZ(1)

T2(I) & T1(I) = transmissivities for either the 6.3μ or 17μ water vapor absorption bands depending on the spectral interval.

T2C(I) & T1C(I) = transmissivities for the 15μ CO_2 absorption band.

T2W(I) & T1W(I) = transmissivities for the H_2O continuum.

T2OZ(I) & T1OZ(I) = transmissivities for the 9.6μ ozone absorption band.

Note: The 2 refers to the present level and the 1 refers to the previous level, therefore, the difference refers to the transmissivity of that layer.

TEBAR = (Text (I) + Text 2 (I))/2 = The average extinction due to aerosols across that layer.

$\overline{TTT3} = \overline{TW} * \overline{TC} * \overline{TCO} * \overline{TO} * \overline{TS} * DTA$

$\overline{TW}$ = The average transmissivity across that layer due to water vapor.
$\overline{TC}$ = The average transmissivity across that layer due to CO_2.
$\overline{TC}$ = The average transmissivity across that layer due to the water vapor continuum.
$\overline{TO}$ = The average transmissivity across that layer due to ozone.
$\overline{TS}$ = The average transmissivity across that layer due to scattering by the aerosols in the layer.
DTA - T2A(I) - T1A(I)
T2A & T1A = Transmissivities of aerosols. The 2 refers to the present level and the 1 refers to the previous level.

Therefore equation (12) is

ΔT = DT (change in T for gas) * TEBAR(T for aerosol) + TTT3 (change in T for aerosol *T (gas))

III. Numerical Techniques Requiring Major Portion of the Computer Time

In the radiation transfer program optical masses (u*) and transmissivities (T) must be calculated for each layer and each 10 wavenumber increment (i.e. 1140ν to 820ν). The values are then used in the total radiance calculation:

$$(13) \quad N_{TOT} = \sum_{\nu 1po}^{\nu 2p} \sum N\nu(T)\Delta T\nu\Delta\nu$$

where

$$N\nu(T) = C_1\nu^3/\pi*(EXP(C_2\nu/T) - 1) - \text{Plank's Law}$$

This equation requires two summations to be performed.(1) A summation over wavenumbers and (2) A summation over layers. In the program this is accomplished by summing over wavenumbers for each layer and then summing the layers.

The calculated radiances from the radiation transfer program are used to determine a profile of radiance versus pressure altitude. This can only be done by calculating the radiance from the atmosphere about the reference level and then moving up to the next reference level (i.e. each 50 mb) and repeating the summation for N_{TOT} with one less level. This must be accomplished for each 50 mb level. On the CSU CDC 6400 computer it takes approximately 68 seconds of CP time to calculate one profile.

A flowchart of the extinction coefficient program is attached. As can be seen from the flow chart two summations must occur. (1) The calculation of the Mie single-particle extinction (Kext) or scattering (Kscat) cross sections as shown in equations (8) & (9) and (2) the calculation of the extinction (B_{EXT}) or scattering (B_{SCAT}) volume cross sections as shown in equation (11). The MIE single-particle extinction and scattering cross section calculations are accomplished in the subroutine crosec. The upper limit of integration is NN - 1.2*x+9.0 which is the value used for the termination of the recursion relations for a_η & b_η, the MIE complex scattering coefficients. The limits of integration used in the volumn cross section calculations are the lower and upper limits of particle size for a given type haze distribution. For a typical maritime haze distribution approximately 30 seconds of CP time is used on the CDC to determine B_{EXT}, B_{SCAT}, and B_{ABS}.

III. RADIANV FLOW DIAGRAM

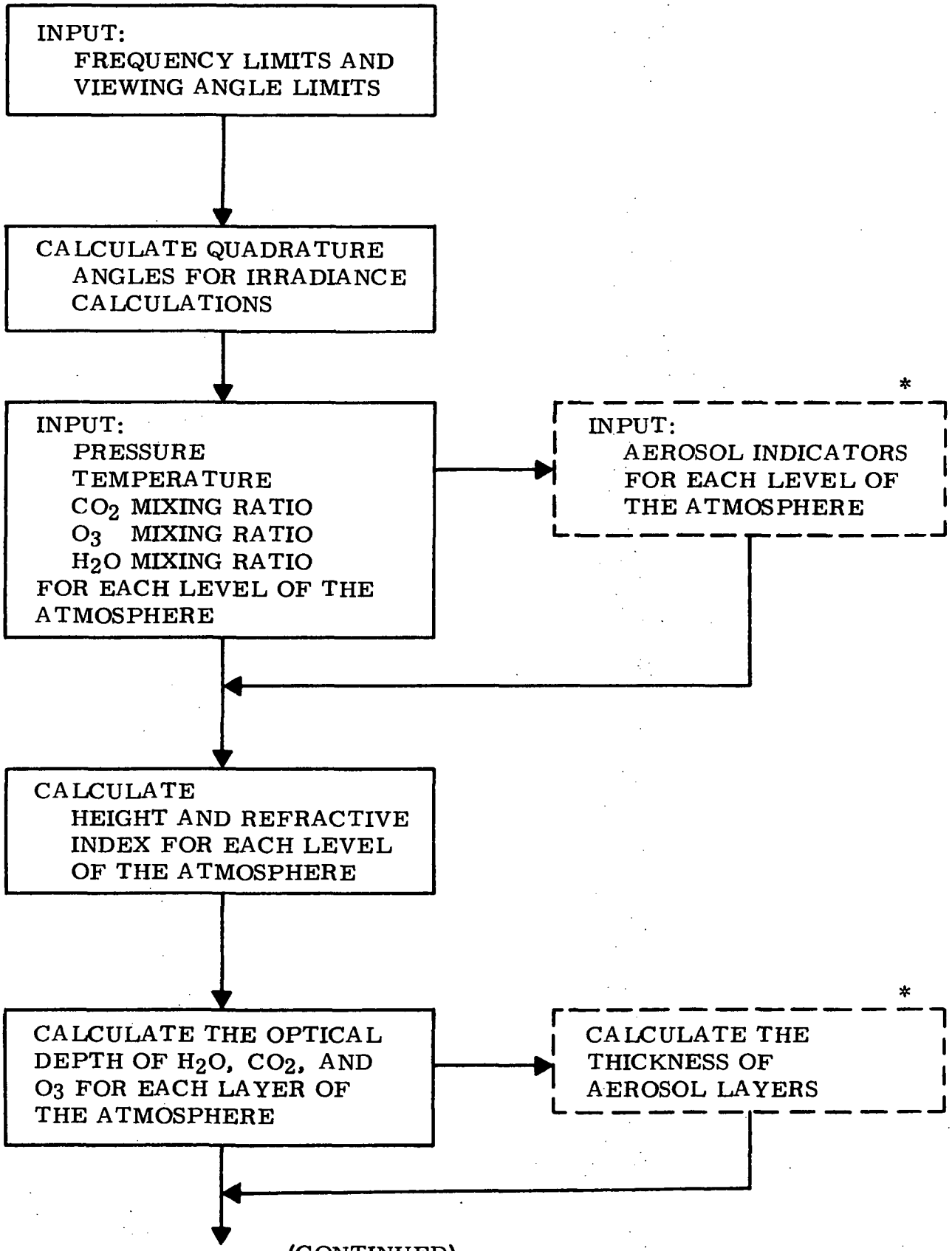

(CONTINUED)

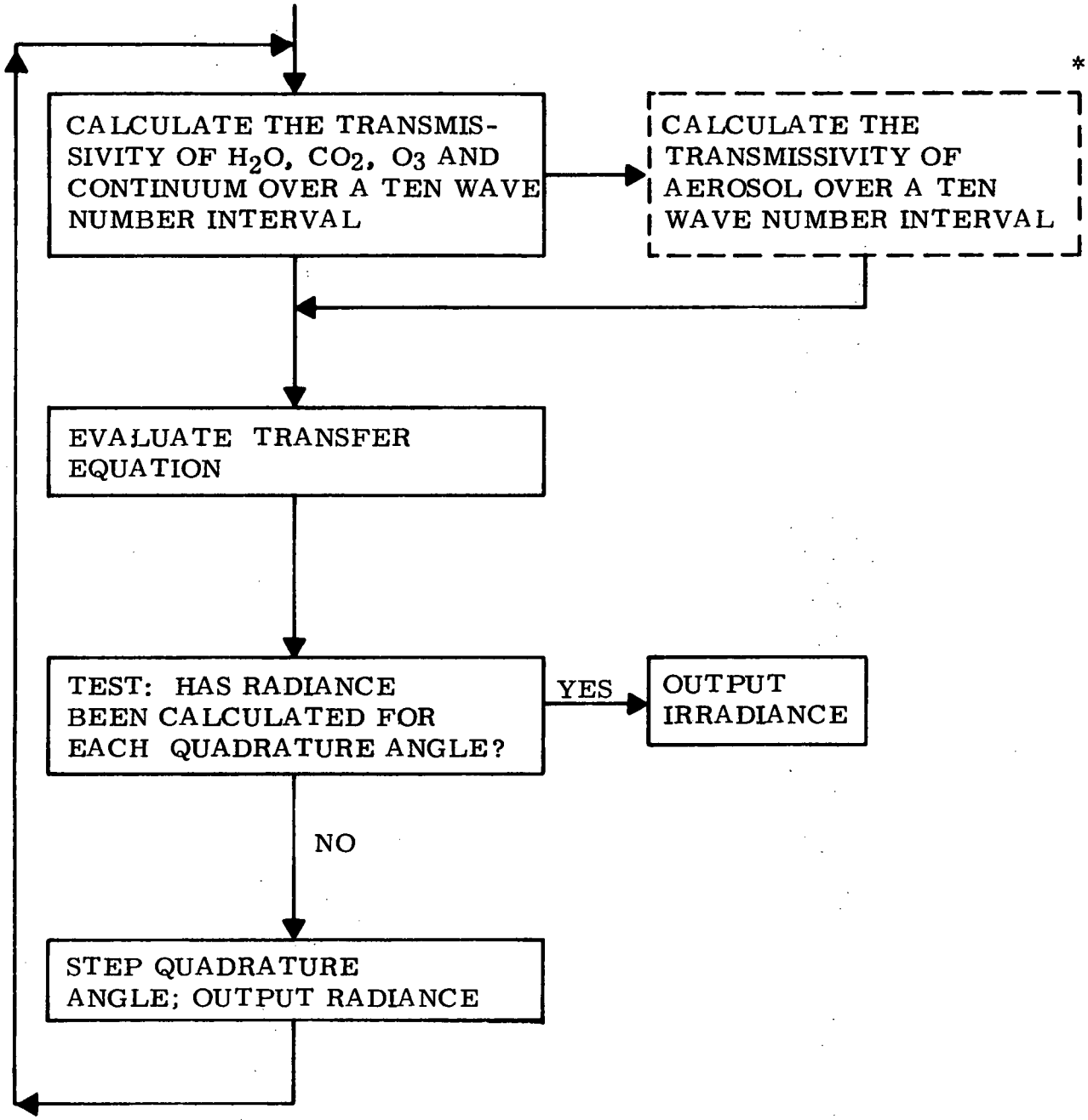

* DASHED LINE BOXES INDICATE ADDITION DUE TO AEROSOLS

IV. EXTCOEF

The purpose of the program EXTCOEF is to provide the extinction, scattering, and absorption volume cross sections for a given particulate or cloud droplet distribution. These volume cross sections are then used in program RADIANV to calculate the role of the given particulate or cloud droplet distribution in the infrared radiation transfer process through the atmosphere. The basis for EXTCOEF can be found in a series of works by D. Deirmendjian (1959, 1960, 1969)* and D. Deirmendjian and R.J. Clasen (1962).

The program takes indices of refraction for several wavelengths across the portion of the infrared spectrum of interest to the user and the particle or droplet size distribution equation from the chosen aerosol or cloud model. It calculates, through Mie theory, the volume cross sections for extinction, scattering, and absorption of illuminating radiation in the portion of the infrared spectrum chosen above.

The calculations are made according to the following procedure:

1) For each wavelength and corresponding index of refraction, the main program calculates the propogation constant, XK; the Mie size parameter, X; and calls SUBROUTINE CROSEC.
2) CROSEC then computes equation (3), K_{EXT}, in the reference "Light Scattering on Partially Homogeneous Spheres of Finite Size" (Deirmendjian, 1962). The recursion relations used in CROSEC are taken from the same reference and the steps are explained in the flow chart for EXTCOEF, section II of this report.

*Bibliography included at the end of Appendix II.

3) Upon the completion of CROSEC, K_{EXT} is returned to the main program as TKSCA and equation (80) in the reference Electromagnetic Scattering on Spherical Polydispersions (Deirmendjian, 1969), is calculated as WTBETA providing the extinction volume cross sections.

4) Each wavelength XLAM, both parts of the refractive index RR and RI, and WTBETA are printed out.

5) Two flags, M and ICHECK, are set--M from 0 to N and ICHECK from 0 to 1--and step 1 is repeated.

6) CROSEC computes equation (4), K_{SC} (Deirmendjian, 1962).

7) K_{SC} is returned to the main program as TKSCA and equation (80) (Deirmendjian, 1969) is again calculated, this time providing scattering volume cross sections as WTBETA.

8) XLAM, RR, RI, and WTBETA are printed out.

9) The absorption volume cross sections are then calculated from the equation XABS(I)=XBEXT(I)-XSCAT(I) where the XBEXT(I) are the extinction values, the XSCAT(I) are the scattering values and XABS(I) are the absorption values.

10) Wavenumber values V(I) corresponding to the wavelength values XLAM(I) are calculated.

11) V(I), XBEXT(I), XBABS(I), and XSCAT(I) are printed out.

The user of EXTCOEF must provide the following information:

1) FXK: an equation of the size distribution of the chosen particulate or cloud model. It gives (according to a total number of particles of all sizes per unit volume and a minimum radius R1 and a maximum radius R2 for particles under the model) the number of particles per unit volume to be

found of any given radius, R. The general form of FXK used by Deirmendjian is $n(R)=aR^{\alpha}\exp(-bR^{\gamma})$ although FXK does not have to be of that form.

2) RR(I), RI(I), and XLAM(I): the complex index of refraction, M, for this program is written $M(I)=RR(I)-iRI(I)$ where RR is the real part and RI is the imaginary part of the refractive index. XLAM is the wavelength at which the material is illuminated. Therefore, XLAM is a wavelength within the wavelength region of interest for which a complex index of refraction is given. Interpolation between given XLAM's is accomplished within EXTCOEF.

EXTCOEF calculates the volume cross sections by equation (80) (Deirmendjian, 1969): $B(M,XLAM;X_1,X_2)=\pi\int_{X_1}^{X_2} X^2(FXK)(K(M,X)DX$ where the B's are as follows:

1) XBEXT, the extinction volume cross section.

2) XBABS, the absorption volume cross section.

3) XSCAT, the scattering volume cross section.

X_1 and X_2 are the Mie size parameters for R1 and R2 where $X=2\pi R/XLAM$. FXK is the size distribution equation, and the K's are the ratios of extinction, scattering, or absorption cross section to the geometrical cross section.

1) K_{EXT}, the ratio for extincation calculated by the program.

2) K_{SC}, the ratio for scattering calculated by the program.

3) K_{ABS}, the ratio for absorption from $K_{EXT}-K_{SC}$.

The accuracy of the volume cross section values given by EXTCOEF depends on three factors:

1) the accuracy of the indices of refraction provided

2) the accuracy of the size distribution equation in depicting the actual distribution observed

3) the accuracy of the assumption that the cloud droplets or particles are homogeneous and spherical. This assumption is more accurate for some uses than for others. For most cloud droplets it is accurate, while for cirrus clouds the shape of the ice crystals is not well represented by spheres. Even in cases such as cirrus clouds, however, the effect of the random orientation of the particles may make the overall accuracy good of the assumption of homogeneity and spherical shape.

V. FLOW CHART FOR EXTCOEF

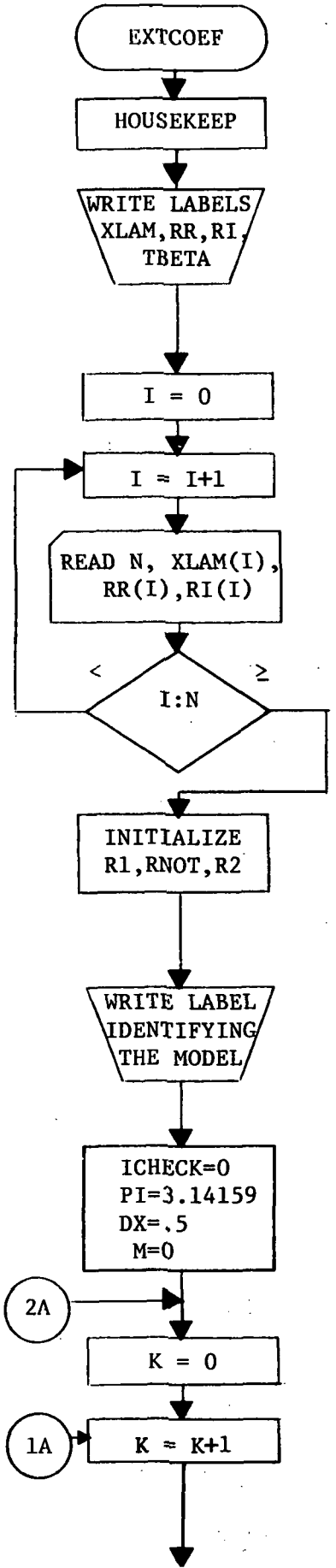

DIMENSION and COMMON statements.

XLAM = wavelength; RR = real part of refractive index at wavelength XLAM; RI = imaginary part of the refractive index; TBETA = the volume cross section for extinction or scattering as defined later.

Initialize index for reading in data.

N = # of wavelengths, XLAM(I), for which an index of refraction, M(I) = RR(I)-iRI(I), will be read in, one data card per wavelength.

R1 and R2 are the minimum and maximum radii, respectively, for the particulate or cloud model chosen. RNOT is a characteristic radius of the model's size distribution and is used mainly to denote a discontinuity of the size distribution equation.

ICHECK is a flag indicating whether extinction or scattering calculations will be made in subroutine CROSEC. DX is the integration increment of size parameter. M is an index used along with ICHECK to differentiate between extinction and scattering calculations.

Initialize index for volume cross section calculations.

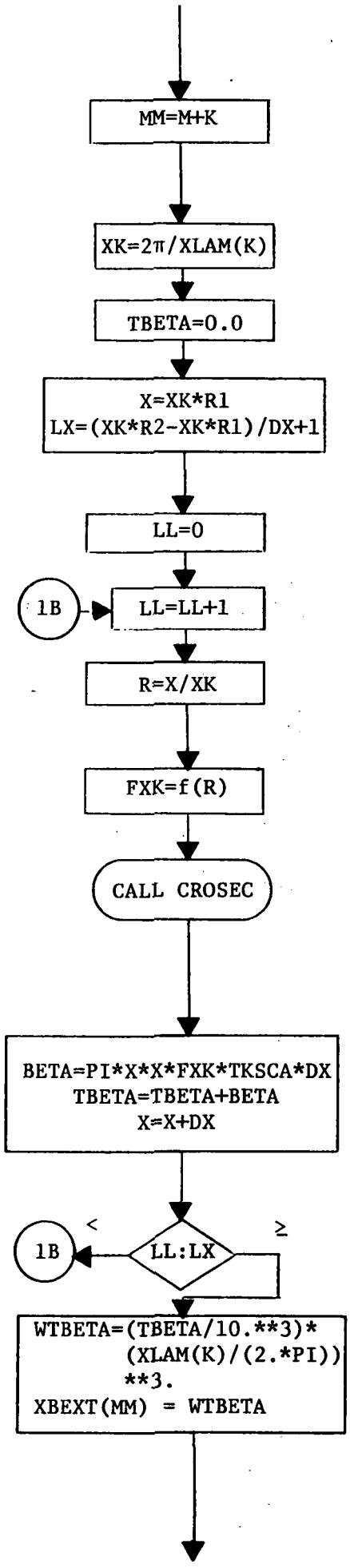

M=0 and ICHECK = 0 for extinction coefficient calculations
M=N and ICHECK = 1 for scattering coefficient calculations.

XK equals the propogation constant.

TBETA is the sum of the integration of BETA.

LX is the # of DX lengths in the size distribution range of interest; thus, the index of summation of the loop.

Initialize the index for the loop.

R is the radius of the particles at that point in the size distribution.

f(R) = size distribution as a function of radius in units of # $cm^{-3}\mu^{-1}$.

CROSEC calculates either $(\frac{2}{X^2})(2n+1)Re\{a_n+b_n\}$ or $(\frac{2}{X^2})(2n+1)\{|a_n|^2+|b_n|^2\}$ depending on ICHECK and M and returns the calculation as TKSCA.

BETA is essentially the volume cross section for a given value of the Mie size parameter X. TBETA is the sum of BETA over the entire range of X. X is incremented by DX during the summation procedure.

WTBETA is the final calculation of extinction or scattering volume cross section for each wavelength XLAM(K). XBEXT(MM) is the indexing of the extinction and scattering volume cross sections in preparation for calculation of the absorption volume cross section.

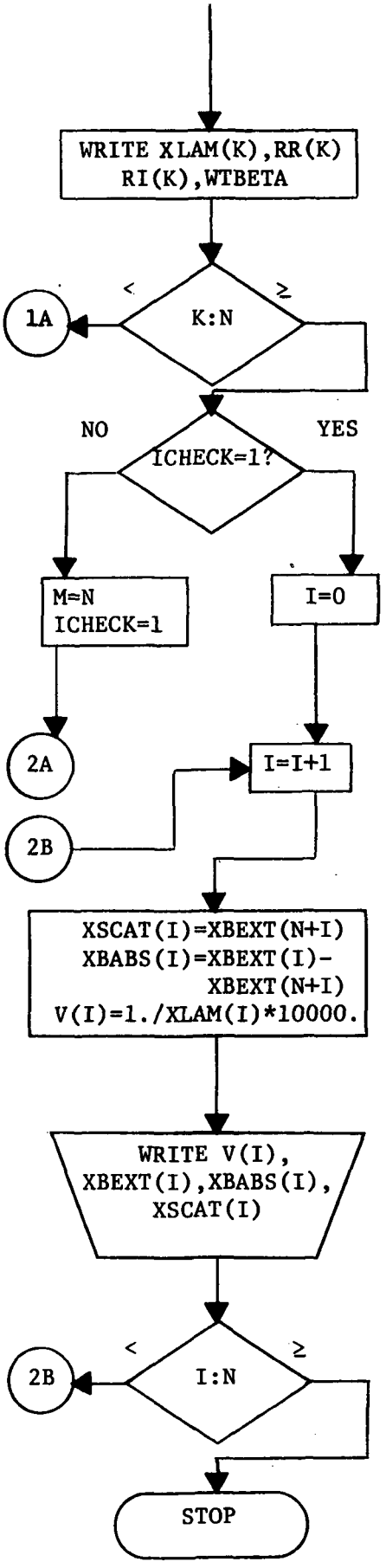

If the extinction cross section calculations are finished, M and ICHECK are reset to N and 1, respectively, and the scattering calculations done. When they are finished, the calculation of absorption volume cross sections are undertaken as follows.

Initialization of the index for the loop.

XSCAT(I) is set for writing out.
XBABS is calculated from the extinction and scattering values. V(I) is the wavenumber corresponding to each wavelength XLAM(I).

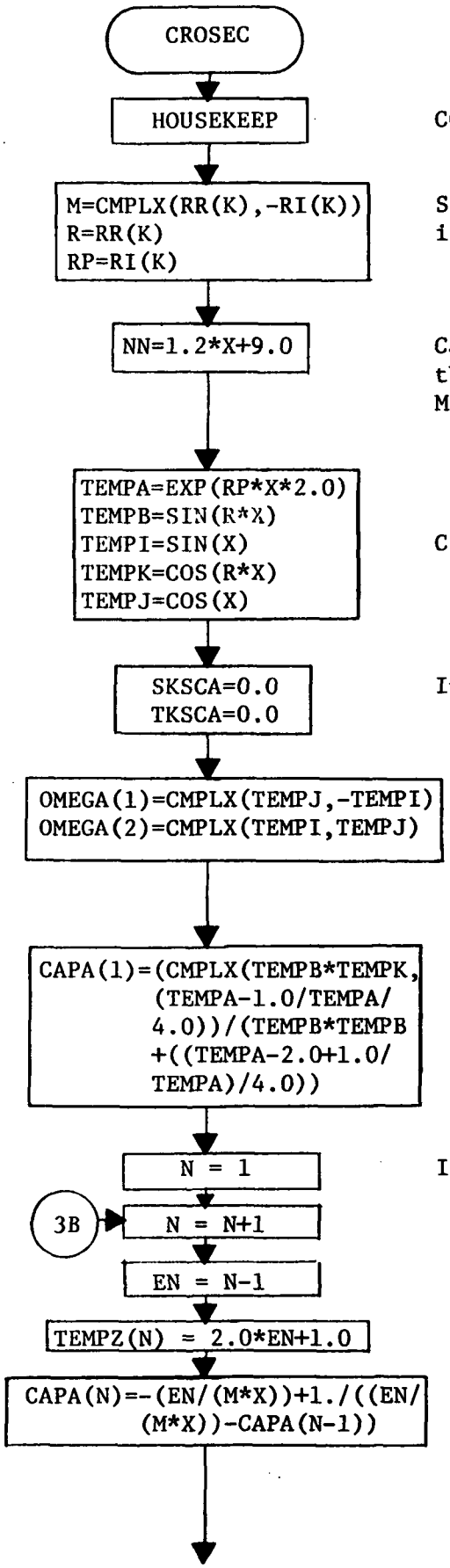

COMPLEX, DIMENSION, and COMMON statements.

Setting of the complex index of refraction and its real and imaginary components.

Calculation of NN, the test for termination of the recursion relations for a_n and b_n, the Mie complex scattering coefficients.

Calculation of factors to be used later.

Initialize the summation parameters.

OMEGA is a function connected with half order Bessel functions. OMEGA(1) and OMEGA(2) are the initial values used in the recursion relation later for OMEGA(N+1).

CAPA(N) is a main parameter in the calculation of a_n and b_n and CAPA(1) is the initial value.

Initialize the index for the loop.

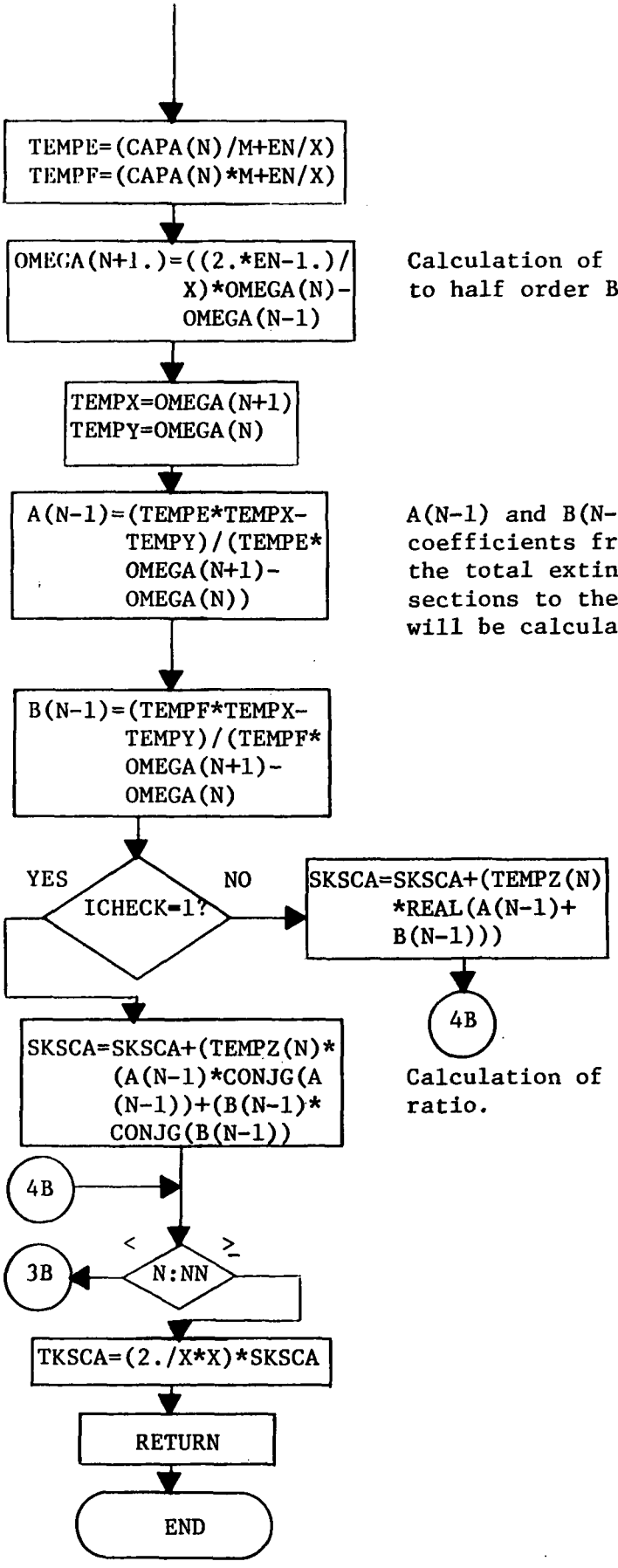

Calculation of the recursion relation corrected to half order Bessel functions.

A(N-1) and B(N-1) are the Mie complex scattering coefficients from which TKSCA, the ratio of the total extinction and scattering cross sections to the geometrical cross sections, will be calculated.

Calculation of the extinction cross section ratio.

Calculation of the scattering cross section ratio.

Appendix I.

APPENDIX I. RADIANV AND EXTCOEF PRINTOUTS

For RADIANV the choice of printout option is made by the symbol in column 80 of the station and date identification card. The name of the variable is IDWT and is either a $, *, or blank. A blank in column 80 will provide the shortest printout of the three. Samples are given below. For all three the wavenumber limits, view angle limits and atmospheric data are printed out. The date of the actual computer run is printed next followed by the words STATION/DATE, and the identification words selected by the user. Next comes VIEWING ANGLE LIMITS in degrees. If this is chosen as 0.00 to 0.00, the integrated irradiance will be 0.0. The next line is an identification of the turbid layer used, if any. WAVELENGTH REGION is the interval in microns over which the integration takes place for the calculations which will follow: for the blank and * option, this is the total wavelength region the user has selected; while the $ option is for 10 wavenumbers within the total interval selected. The same holds for WAVENUMBERS except that the units are cm^{-1}.

The calculated data are given as follows: for all three options the atmospheric data for the reference level is printed, followed by a statement as to whether Elsasser or Smith data were used for the H_2O rotational band and for CO_2. The blank option then prints the ATMOSPHERIC EMISSION TERM for the atmosphere for the wavelength region stated previously. The number must be multiplied

by 10 and the sign changed in order to come up with the correct units of watts cm^{-2} $steradian^{-1}$. For upflux calculations a SURFACE TRANSMISSION TERM is also given which must be multipied by 10. For downflux calculations the SURFACE term is ignored. The next line of data is the look angle for the calculation, the radiance value in watts cm^{-2} $steradian^{-1}$, total cm of CO_2, cm H_2O, cm O_3, and km. of aerosol. The last line of data for the section of data is INTEGRATED IRRADIANCE in watts cm^{-2}.

The * option differs from the blank option in that data are printed out for each layer between the reference layer and the top of the atmosphere. These data are placed after the comment on SMITH or ELSASSER tables. The format of the data is: the average pressure; the DT/DenP; the Planck function time DT; the fraction of the total affect caused by W(water), C(CO_2), O(ozone), and A(aerosols); followed by weighting functions for WWW(water), CCC(CO_2), and OOO(ozone).

The printout for the $ option has the same format as that for the * option. The difference between the two is that the * option calculates the radiance and other data for the total selected wavelength region at once, then drops off one layer of the atmosphere and repeats the operation for the remaining atmosphere. The $ option calculates the radiance and other data for each 10 wavenumbers across the total interval for the entire atmosphere selected and then stops. The blank option drops off layers the same as the * option.

The output of the computer program EXTCOEF is illustrated on the sample output included in this section and is described as follows: XLAM is the wavelength η for which the user supplies the complex refractive indices values. RR is the real part of the refractive index and RI is the imaginary part. TBETA is a label under which two sets of data are printed: under the XLAM column the wavelengths supplied by the user are printed twice and the Beta or volume extinction cross section corresponds to the first set TBETA; the volume scattering cross section corresponds to the second set.

The next series of unlabeled data is a column of a wavenumber corresponding to each original XLAM and then three columns of volume cross sections for those wavenumbers. The order for the cross sections is XBEXT (extinction), XBABS (absorption), and XSCAT (scattering).

The last section of 229 values is identical to that punched on cards to be used in RADIANV except that labels are included on the punched data cards. The left hand column corresponds to wavenumbers and the other three columns are the same as stated in the previous paragraph. The punched deck is divided into three sections of data statements: the first for BABS values, the second for BEXT values, and the third for BSCAT values.

SAMPLE OF BLANK OPTION PRINTOUT

```
DATE - 10/14/70
STATION/DATE, DISC 7713
VIEWING ANGLE LIMITS FROM  -1.00 TO   1.00 DEGREES
MARITIME 100 PARTICLES/CU CM DEIRMENDJIAN
WAVE LENGTH REGION=  7.93651 TO 14.28571 MICRONS  FILTER
WAVE NUMBERS=   700.00 TO  1260.00

PRESSURE  782.0   TEMP.   13.5   MIX RATIO  2.3000   DELU   .1929

 ANGLE   RADIANCE   CM CO2          CM H2O          CM O3     KM AEROSOL

 ZO EQUALS  -.6364473E+04

                    SMITH TABLES FOR H2O FOR ROTATIONAL BAND
                    SMITH TABLES FOR CO2
 ATMOSPHERIC EMISSION TERM =  -.452E+01  SURFACE TRANSMISSION TERM =   .472E+00
   .11  49.898159     51.0497          1.8393          .0012          0.0000
 ZO EQUALS  -.6317990E+04

                    SMITH TABLES FOR H2O FOR ROTATIONAL BAND
                    SMITH TABLES FOR CO2
 ATMOSPHERIC EMISSION TERM =  -.452E+01  SURFACE TRANSMISSION TERM =   .472E+00
   .50  49.898082     51.0518          1.8393          .0012          0.0000
 ZO EQUALS  -.6271510E+04

                    SMITH TABLES FOR H2O FOR ROTATIONAL BAND
                    SMITH TABLES FOR CO2
 ATMOSPHERIC EMISSION TERM =  -.452E+01  SURFACE TRANSMISSION TERM =   .472E+00
   .89  49.897908     51.0567          1.8395          .0012          0.0000

 INTEGRATED IRRADIANCE=      .047729

*******************************************************************************
PRESSURE  842.0   TEMP.   17.0   MIX RATIO  4.0000   DELU   .3888

 ANGLE   RADIANCE   CM CO2          CM H2O          CM O3     KM AEROSOL

 ZO EQUALS  -.6364473E+04

                    SMITH TABLES FOR H2O FOR ROTATIONAL BAND
                    SMITH TABLES FOR CO2
 ATMOSPHERIC EMISSION TERM =  -.454E+01  SURFACE TRANSMISSION TERM =   .537E+00
   .11  50.769969     38.5891          1.6820          .0008          0.0000

 INTEGRATED IRRADIANCE=      .047781

*******************************************************************************
PRESSURE  902.0   TEMP.   17.2   MIX RATIO  8.7000   DELU   .1919

 ANGLE   RADIANCE   CM CO2          CM H2O          CM O3     KM AEROSOL

 ZO EQUALS  -.6364473E+04

                    SMITH TABLES FOR H2O FOR ROTATIONAL BAND
                    SMITH TABLES FOR CO2
 ATMOSPHERIC EMISSION TERM =  -.449E+01  SURFACE TRANSMISSION TERM =   .710E+00
```

SAMPLE OF * OPTION PRINTOUT

```
 DATE-- 06/04/71
STATION/DATE- DISC 7/23
VIEWING ANGLE LIMITS FROM   0.00 TO   0.00 DEGREES
MARITIME 100 PARTICLES/CU CM DEIRMENDJIAN
WAVE LENGTH REGION=  7.93651 TO 14.28571 MICRONS  FILTER
WAVE NUMBERS=   700.00 TO  1260.00

PRESSURE  658.0   TEMP.    4.5   MIX RATIO 1.6000   DELU   .0253

                  SMITH TABLES FOR H20 FOR ROTATIONAL BAND
                  SMITH TABLES FOR CO2
 PBAR 665.5 DTAU/DLNP*7.042 B(U,T)*DT  .670E+00 W  .66E+00 C 0.     0 0.     A  .33E+00 WWW  .25E-01 CCC  .36E+01 000  .14E-03
 PBAR 686.5 DTAU/DLNP*1.703 B(U,T)*DT  .693E+00 W  .56E+00 C 0.     0 0.     A  .40E+00 WWW  .52E-01 CCC  .65E+01 000  .24E-03
 PBAR 727.5 DTAU/DLNP*6.959 B(U,T)*DT  .104E+01 W  .57E+00 C 0.     0 0.     A  .34E+00 WWW  .14E+00 CCC  .13E+02 000  .45E-03
 PBAR 740.0 DTAU/DLNP*0.526 B(U,T)*DT  .165E+00 W  .63E+00 C 0.     0 0.     A  .26E+00 WWW  .39E-01 CCC  .24E+01 000  .75E-04
 PBAR 768.5 DTAU/DLNP*5.702 B(U,T)*DT  .131E+00 W  .71E+00 C 0.     0 0.     A  .19E+00 WWW  .40E-01 CCC  .17E+01 000  .51E-04
 PBAR 788.5 DTAU/DLNP*8.066 B(U,T)*DT  .551E+00 W  .75E+00 C 0.     0 0.     A  .16E+00 WWW  .25E+00 CCC  .80E+01 000  .23E-03
 PBAR 827.5 DTAU/DLNP*1.515 B(U,T)*DT  .487E+00 W  .76E+00 C 0.     0 0.     A  .13E+00 WWW  .44E+00 CCC  .11E+02 000  .29E-03
 PBAR 865.5 DTAU/DLNP*1.004 B(U,T)*DT  .209E+00 W  .79E+00 C 0.     0 0.     A  .99E-01 WWW  .38E+00 CCC  .75E+01 000  .18E-03
 PBAR 940.5 DTAU/DLNP*5.231 B(U,T)*DT  .286E+00 W  .77E+00 C 0.     0 0.     A  .85E-01 WWW  .17E+01 CCC  .29E+02 000  .59E-03
 PBAR1008.5 DTAU/DLNP* 7.650 B(U,T)*DT  .132E-01 W  .83E+00 C 0.     0 0.     A  .47E-01 WWW  .29E+00 CCC  .41E+01 000  .57E-04
 ATMOSPHERIC EMISSION TERM =  -.425E+01  SURFACE TRANSMISSION TERM =   .407E-01
ANGLE   RADIANCE   CM CO2        CM H20        CM 03      KM AEROSOL

  0.00  42.883297     86.8047        2.9228        .0022        2.9537
**********************************************************************************************************************

INTEGRATED IRRADIANCE=    0.000000

**********************************************************************************************************************
PRESSURE  673.0   TEMP.    4.6   MIX RATIO 1.7000   DELU   .0523

                  SMITH TABLES FOR H20 FOR ROTATIONAL BAND
                  SMITH TABLES FOR CO2
 PBAR 686.5 DTAU/DLNP*3.669 B(U,T)*DT  .106E+01 W  .65E+00 C 0.     0 0.     A  .33E+00 WWW  .52E-01 CCC  .65E+01 000  .24E-03
 PBAR 727.5 DTAU/DLNP*3.058 B(U,T)*DT  .121E+01 W  .58E+00 C 0.     0 0.     A  .35E+00 WWW  .14E+00 CCC  .13E+02 000  .45E-03
 PBAR 760.0 DTAU/DLNP*9.455 B(U,T)*DT  .186E+00 W  .64E+00 C 0.     0 0.     A  .26E+00 WWW  .39E-01 CCC  .24E+01 000  .75E-04
 PBAR 768.5 DTAU/DLNP*6.911 B(U,T)*DT  .147E+00 W  .72E+00 C 0.     0 0.     A  .20E+00 WWW  .40E-01 CCC  .17E+01 000  .51E-04
 PBAR 788.5 DTAU/DLNP*5.546 B(U,T)*DT  .613E+00 W  .75E+00 C 0.     0 0.     A  .17E+00 WWW  .25E+00 CCC  .80E+01 000  .23E-03
 PBAR 827.5 DTAU/DLNP*1.824 B(U,T)*DT  .535E+00 W  .77E+00 C 0.     0 0.     A  .13E+00 WWW  .44E+00 CCC  .11E+02 000  .29E-03
 PBAR 865.5 DTAU/DLNP*7.018 B(U,T)*DT  .228E+00 W  .79E+00 C 0.     0 0.     A  .10E+00 WWW  .38E+00 CCC  .75E+01 000  .18E-03
 PBAR 940.5 DTAU/DLNP*2.238 B(U,T)*DT  .310E+00 W  .77E+00 C 0.     0 0.     A  .89E-01 WWW  .17E+01 CCC  .29E+02 000  .59E-03
 PBAR1008.5 DTAU/DLNP* 8.245 B(U,T)*DT  .143E-01 W  .83E+00 C 0.     0 0.     A  .49E-01 WWW  .29E+00 CCC  .41E+01 000  .57E-04
 ATMOSPHERIC EMISSION TERM =  -.430E+01  SURFACE TRANSMISSION TERM =   .442E-01
ANGLE   RADIANCE   CM CO2        CM H20        CM 03      KM AEROSOL

  0.00  43.399959     83.1777        2.9050        .0021        2.8327
**********************************************************************************************************************

INTEGRATED IRRADIANCE=    0.000000

**********************************************************************************************************************
PRESSURE  700.0   TEMP.    6.8   MIX RATIO 2.1000   DELU   .1445

                  SMITH TABLES FOR H20 FOR ROTATIONAL BAND
                  SMITH TABLES FOR CO2
 PBAR 727.5 DTAU/DLNP*0.751 B(U,T)*DT  .192E+01  .66E+00 C 0.     0 0.     A  .31E+00 WWW  .14E+00 CCC  .13E          .3E 03
```

SAMPLE OF # OPTION PRINTOUT

```
DATE - 10/16/70
STATION/DATE, DISC 7/18
VIEWING ANGLE LIMITS FROM  -1.00 TO   1.00 DEGREES
MARITIME 100 PARTICLES/CU CM DEIRMENDJIAN
WAVE LENGTH REGION= 13.79310 TO 13.98601 MICRONS  FILTER
WAVE NUMBERS=   715.00 TO   725.00

PRESSURE  644.0   TEMP.    7.4   MIX RATIO  1.7000   DELU   .1212

 Z0 EQUALS  -.6364473E+04

                  SMITH TABLES FOR H20 FOR ROTATIONAL BAND
                  SMITH TABLES FOR C02
 PBAR 671.0 DTAU/DLNP 8.284 B(U,T)*DT  .768E-01 W  .36E-01 C  .96E+00 0 0.     A 0.     WWW  .12E+00 CCC  .13E+02 000  .48E-03
 PBAR 745.0 DTAU/DLNP 1.542 B(U,T)*DT  .237E-01 W  .96E-01 C  .90E+00 0 0.     A 0.     WWW  .26E+00 CCC  .23E+02 000  .74E-03
 PBAR 817.0 DTAU/DLNP  .763 B(U,T)*DT  .594E-02 W  .24E+00 C  .76E+00 0 0.     A 0.     WWW  .30E+00 CCC  .12E+02 000  .33E-03
 PBAR 873.0 DTAU/DLNP  .544 B(U,T)*DT  .508E-02 W  .38E+00 C  .62E+00 0 0.     A 0.     WWW  .60E+00 CCC  .15E+02 000  .36E-03
 PBAR 929.5 DTAU/DLNP  .368 B(U,T)*DT  .276E-02 W  .47E+00 C  .53E+00 0 0.     A 0.     WWW  .63E+00 CCC  .12E+02 000  .26E-03
 PBAR 975.5 DTAU/DLNP  .263 B(U,T)*DT  .156E-02 W  .53E+00 C  .47E+00 0 0.     A 0.     WWW  .59E+00 CCC  .99E+01 000  .19E-03
 PBAR1005.0 DTAU/DLNP  .219 B(U,T)*DT  .573E-03 W  .59E+00 C  .41E+00 0 0.     A 0.     WWW  .31E+00 CCC  .44E+01 000  .60E-04
 ATMOSPHERIC EMISSION TERM =  -.116E+00  SURFACE TRANSMISSION TERM =   .271E-02
 ANGLE    RADIANCE    CM C02          CM H20          CM 03      KM AEROSOL

   .11   1.190375      77.4005         2.4609          .0024       0.0000

 INTEGRATED IRRADIANCE=       .001154

**********************************************************************************************************************************
```



```
DATE - 10/16/70
STATION/DATE, DISC 7/18
VIEWING ANGLE LIMITS FROM  -1.00 TO   1.00 DEGREES
MARITIME 100 PARTICLES/CU CM DEIRMENDJIAN
WAVE LENGTH REGION= 13.60544 TO 13.79310 MICRONS  FILTER
WAVE NUMBERS=   725.00 TO   735.00

PRESSURE  644.0   TEMP.    7.4   MIX RATIO  1.7000   DELU   .1212

 Z0 EQUALS  -.6364473E+04

                  SMITH TABLES FOR H20 FOR ROTATIONAL BAND
                  SMITH TABLES FOR C02
 PBAR 671.0 DTAU/DLNP 3.920 B(U,T)*DT  .359E-01 W  .20E+00 C  .80E+00 0 0.     A 0.     WWW  .12E+00 CCC  .13E+02 000  .48E-03
 PBAR 745.0 DTAU/DLNP 2.052 B(U,T)*DT  .311E-01 W  .26E+00 C  .74E+00 0 0.     A 0.     WWW  .26E+00 CCC  .23E+02 000  .74E-03
 PBAR 817.0 DTAU/DLNP 1.772 B(U,T)*DT  .137E-01 W  .43E+00 C  .57E+00 0 0.     A 0.     WWW  .30E+00 CCC  .12E+02 000  .33E-03
 PBAR 873.0 DTAU/DLNP 1.579 B(U,T)*DT  .146E-01 W  .55E+00 C  .45E+00 0 0.     A 0.     WWW  .60E+00 CCC  .15E+02 000  .36E-03
 PBAR 929.5 DTAU/DLNP 1.211 B(U,T)*DT  .901E-02 W  .59E+00 C  .41E+00 0 0.     A 0.     WWW  .63E+00 CCC  .12E+02 000  .26E-03
 PBAR 975.5 DTAU/DLNP  .939 B(U,T)*DT  .552E-02 W  .62E+00 C  .38E+00 0 0.     A 0.     WWW  .59E+00 CCC  .99E+01 000  .19E-03
 PBAR1005.0 DTAU/DLNP  .829 B(U,T)*DT  .215E-02 W  .65E+00 C  .35E+00 0 0.     A 0.     WWW  .31E+00 CCC  .44E+01 000  .60E-04
 ATMOSPHERIC EMISSION TERM =  -.112E+00  SURFACE TRANSMISSION TERM =   .124E-01
 ANGLE    RADIANCE    CM C02          CM H20          CM 03      KM AEROSOL

   .11   1.243984      77.4005         2.4609          .0024       0.0000

 INTEGRATED IRRADIANCE=       .001157

**********************************************************************************************************************************
```

SAMPLE OF EXTCOEF PRINTOUT

XLAM	RR	RI	TBETA
	7/23 QUARTZ HAZE		
15.000	1.330	.430	.239095E-02
14.000	1.275	.358	.353830E-02
13.500	1.245	.320	.418556E-02
13.000	1.220	.292	.501190E-02
12.500	1.190	.244	.547778E-02
12.000	1.160	.209	.610864E-02
11.500	1.145	.153	.575518E-02
11.000	1.151	.102	.490866E-02
10.500	1.185	.069	.421661E-02
10.000	1.214	.053	.411881E-02
9.500	1.245	.044	.428027E-02
9.000	1.269	.040	.499949E-02
8.500	1.286	.038	.578383E-02
8.000	1.293	.036	.677593E-02
7.500	1.303	.035	.793947E-02
15.000	1.330	.430	.828685E-04
14.000	1.275	.358	.101574E-03
13.500	1.245	.320	.106852E-03
13.000	1.220	.292	.115160E-03
12.500	1.190	.244	.107483E-03
12.000	1.160	.209	.101317E-03
11.500	1.145	.153	.833988E-04
11.000	1.151	.102	.793742E-04
10.500	1.185	.069	.117011E-03
10.000	1.214	.053	.181950E-03
9.500	1.245	.044	.286036E-03
9.000	1.269	.040	.442292E-03
8.500	1.286	.038	.619674E-03
8.000	1.293	.036	.810549E-03
7.500	1.303	.035	.108262E-02

666.66667	.239095E-02	.230808E-02	.828685E-04
714.28571	.353830E-02	.343673E-02	.101574E-03
740.74074	.418556E-02	.407871E-02	.106852E-03
769.23077	.501190E-02	.489674E-02	.115160E-03
800.00000	.547778E-02	.537030E-02	.107483E-03
833.33333	.610864E-02	.600732E-02	.101317E-03
869.56522	.575518E-02	.567178E-02	.833988E-04
909.09091	.490866E-02	.482929E-02	.793742E-04
952.38095	.421661E-02	.409960E-02	.117011E-03
1000.00000	.411881E-02	.393686E-02	.181950E-03
1052.63158	.428027E-02	.399423E-02	.286036E-03
1111.11111	.499949E-02	.455720E-02	.442292E-03
1176.47059	.578383E-02	.516415E-02	.619674E-03
1250.00000	.677593E-02	.596538E-02	.810549E-03
1333.33333	.793947E-02	.685685E-02	.108262E-02

0.00000	0.	0.	0.
10.00000	0.	0.	0.
20.00000	0.	0.	0.
30.00000	0.	0.	0.
40.00000	0.	0.	0.
50.00000	0.	0.	0.
60.00000	0.	0.	0.
70.00000	0.	0.	0.
80.00000	0.	0.	0.
90.00000	0.	0.	0.
100.00000	0.	0.	0.
110.00000	0.	0.	0.
120.00000	0.	0.	0.
130.00000	0.	0.	0.
140.00000	0.	0.	0.
150.00000	0.	0.	0.
160.00000	0.	0.	0.
170.00000	0.		

170.00000	0.	0.	0.
180.00000	0.	0.	0.
190.00000	0.	0.	0.
200.00000	0.	0.	0.
210.00000	0.	0.	0.
220.00000	0.	0.	0.
230.00000	0.	0.	0.
240.00000	0.	0.	0.
250.00000	0.	0.	0.
260.00000	0.	0.	0.
270.00000	0.	0.	0.
280.00000	0.	0.	0.
290.00000	0.	0.	0.
300.00000	0.	0.	0.
310.00000	0.	0.	0.
320.00000	0.	0.	0.
330.00000	0.	0.	0.
340.00000	0.	0.	0.
350.00000	0.	0.	0.
360.00000	0.	0.	0.
370.00000	0.	0.	0.
380.00000	0.	0.	0.
390.00000	0.	0.	0.
400.00000	0.	0.	0.
410.00000	0.	0.	0.
420.00000	0.	0.	0.
430.00000	0.	0.	0.
440.00000	0.	0.	0.
450.00000	0.	0.	0.
460.00000	0.	0.	0.
470.00000	0.	0.	0.
480.00000	0.	0.	0.
490.00000	0.	0.	0.
500.00000	0.	0.	0.
510.00000	0.	0.	0.
520.00000	0.	0.	0.
530.00000	0.	0.	0.
540.00000	0.	0.	0.
550.00000	0.	0.	0.
560.00000	0.	0.	0.
570.00000	0.	0.	0.
580.00000	0.	0.	0.
590.00000	0.	0.	0.
600.00000	0.	0.	0.
610.00000	0.	0.	0.
620.00000	0.	0.	0.
630.00000	0.	0.	0.
640.00000	0.	0.	0.
650.00000	0.	0.	0.
660.00000	0.	0.	0.
670.00000	.247127E-02	.238709E-02	.841778E-04
680.00000	.271221E-02	.262410E-02	.881060E-04
690.00000	.295315E-02	.286112E-02	.920342E-04
700.00000	.319410E-02	.309814E-02	.959623E-04
710.00000	.343504E-02	.333515E-02	.998905E-04
720.00000	.367811E-02	.357540E-02	.102714E-03
730.00000	.392278E-02	.381807E-02	.104709E-03
740.00000	.416744E-02	.406074E-02	.106704E-03
750.00000	.445412E-02	.434457E-02	.109552E-03
760.00000	.474417E-02	.463170E-02	.112468E-03
770.00000	.502355E-02	.490858E-02	.114968E-03
780.00000	.517496E-02	.506249E-02	.112473E-03
790.00000	.532637E-02	.521639E-02	.109978E-03
800.00000	.547779E-02	.537030E-02	.107483E-03
810.00000	.566704E-02	.556141E-02	.105633E-03

Appendix II.

APPENDIX II. COMPUTED AND CALCULATED INFRARED TRANSFER THROUGH CLEAR AND HAZY ATMOSPHERES*

A STUDY OF THE ATTENUATION BY ATMOSPHERIC PARTICULATES OF THERMAL INFRARED RADIATION

William E. Marlatt
James C. Harlan

Colorado State University
Fort Collins, Colorado

ABSTRACT

In July, 1969, investigators from Colorado State University participated in the Barbados Oceanographic and Meteorological Experiment. The University aircraft flew in conjunction with the NASA Convair 990 on a series of underflights of the NIMBUS III in order to monitor the concentrations of atmospheric particulates and the brightness temperature of the sea surface. The objective of the research program by the authors was to evaluate the role of the atmospheric particulates in the attenuation of infrared radiation by the atmosphere.

After computer simulation of the atmospheric attenuation by molecular atmospheric constituents alone, comparisons were made between the calculated values of brightness temperature and the values observed by the aircraft-borne radiometer and the NIMBUS III MRIR 10-11 micron bandpass channel. Although the calculated values were within 7% of measured values for a case where very low concentrations of atmospheric aerosols were observed, they differed by nearly 20% for a condition of high concentrations of particulate matter in the atmosphere. The aerosol effect has been determined quantitatively to be as significant in infrared remote sensing as low cloud layers.

---

1. INTRODUCTION

As early as 1964 (Marlatt, 1964), research programs to determine the atmospheric attenuation of infrared energy had pointed out the effect of atmospheric particulates on infrared remote sensing from aircraft and satellites. Under sky conditions noted by ground observers as clear, radiometer measurements by aircraft and satellite-borne radiometers over the Pawnee Grasslands of Colorado indicated much higher attenuation by the atmosphere than could be accounted for by molecular constituents alone. In one case of satellite measurements nearly transparent cirrus layers could account for the anomolous attenuation. For other cases involving aircraft measurements, however, only atmospheric haze layers could be determined to be the cause.

During the past four years aerosol counters were added to the Colorado State University and NASA aircraft for satellite underflight programs. This paper discusses the results of a program involving measurements using the CSU Aero Commander and the NASA Convair 990 in conjunction with the Barbados Oceanographic and Meteorological Experiment (BOMEX).

*Paper presented by W.E. Marlatt and J.C. Harlan at the Seventh International Symposium on Remote Sensing of the Environment, May, 1971.

During June and July, 1969, the Colorado State University aircraft, a twin-engined Aero Commander 500B, was in Barbados to monitor various atmospheric parameters and the sea surface temperature. During July the Aero Commander was flown in conjunction with the NASA Convair 990 which carried a second experiment package from Colorado State University. In this period the primary role of the Aero Commander was to measure atmospheric particulates, sea surface temperature, and other atmospheric parameters on flights along the NIMBUS III ground track in the BOMEX area. At the same time atmospheric particulates were also measured on the Convair 990.

The study of the role of aerosols in the observation of sea surface temperature by radiometer permits quantitative correction of the attenuation of the infrared energy in its transfer from the surface through the atmosphere. The use of a radiometer allows no capability for identification of surface features by spatial configuration. In cases where other than differences in temperature with space or time are required by an experiment, therefore, it is necessary to be able to correct the observed radiometric temperatures for atmospheric attenuation in order to determine the exact brightness temperature of the radiating surface. Much work has been done concerning the effects of gaseous atmospheric constituents (Goody, 1964; Kondrat'yev, 1969; Wolfe, 1965) on infrared radiation transfer, and, as will be seen later in this paper, excellent agreement has been obtained by the authors between computed and observed apparent sea surface temperatures for cases of clear, haze-free skies. Good research has been done in the determination of concentrations of atmospheric particulates and their size distributions (Davies, 1966; Junge, 1963; Reeser, 1969).

The problem of the effect of atmospheric particulates on infrared radiation transfer has not been solved although notable work as been done (Deirmendjian, 1959, 1964, 1969; Marlatt, 1965; Peterson, 1968). The objective of the present and future research by the authors is to produce computer simulation of the atmosphere including particulate matter in order to accurately correct the observed radiometric temperature for the total attenuation by the atmosphere. The aerosol simulation requires the solution of two major problems: first, accurate laboratory data on the refractive indices of the particulate materials found in the atmosphere are often not available; and second, the Mie scattering for shapes other than spherical or for non-homogeneous particles is so complex that it has not been solved except for a few special cases, none of which is directly applicable to the atmosphere.

2. DATA ACQUISITION AND ANALYSIS

Two types of aerosol counters were used by Colorado State University to monitor atmospheric particulates. On both the Aero Commander and the Convair 990 a Bausch and Lomb model 40-1 Dust Counter monitored the concentration of particles with diameters equal to or greater than 0.3 microns. The Bausch and Lomb instrument is an electro-optical counter utilizing the light which is scattered in the forward direction by the particles in an illuminated sample of air. The operation is a continuous process, with 170 milliliters of air passing through the instrument per minute. Several size ranges of particles can be counted by this instrument giving a capability for determining particle size distribution for the large atmospheric particles. The instrument counts all particles of diameter as large or larger than the diameter selected--that is, as large or larger than 0.3, 0.5, 1.0, 1.8, 2.0, 3.0, 5.0, or 10.0 microns.

A General Electric Condensation Nuclei Counter was also used aboard the NASA Convair 990 during the last few flights of the BOMEX program. The Condensation Nuclei Counter counted all particles with diameter between approximately 0.002 and 0.4 microns. The Condensation Nuclei Counter operates in the following manner: a sample of air is drawn into an expansion chamber where rapid expansion causes condensation to take place on the nuclei. These nuclei grow rapidly until

they reach approximately 5.0 microns diameter. At the end of the time required for this growth, approximately 26 milliseconds, the light scattered in a forward direction by the particles in the chamber is transformed into a voltage output proportionate to the number of particles viewed. The sampling rate for this instrument is 5 samples per second.

An iso-kinetic flow intake system was designed in which the intake nozzle extended out past the boundary layer of the aircraft. Because of the pressurization system of the aircraft in the case of the Convair 990, special measures were taken to assure that the aerosol measuring system was airtight. In the Aero Commander, which is not pressurized, such measures were not necessary.

The Aero Commander carried a Barnes PRT-5 Infrared Radiometer to monitor the apparent sea surface temperature. This instrument had a standard 8-14 micron wavelength bandpass filter with a 2^{o} field-of-view. The instrument was mounted looking vertically downward through a large camera port behind the co-pilot's seat. Infrared energy incident on the radiometer's detector is electronically changed to a voltage output proportional to the brightness temperature of the surface being observed. The outputs of the particle counters and radiometer were recorded on magnetic tape and processed later at Colorado State University.

Not all the data utilized for this paper came from the instruments aboard the Colorado State University and NASA aircraft in BOMEX. Figure 1 shows the BOMEX ship and aircraft array for most of the experiment. The USC & GSS Discoverer was at position Echo during the entire period. From it radiosonde and sea surface temperature data were obtained at frequent intervals. These were used as input into RADIANV along with any and all available aircraft data. The cases discussed in section 5 describe conditions which existed in the vicinity of the Discoverer and all three cases are for data obtained near 1500 universal time which was the time of one of the regular radiosonde ascents from the ships.

From figure 1 one can determine the flight track of the aircraft when making vertical ascents or descents (profiles) for the indicated day, July 18. In this case the aircraft used for these profiles was the NASA Convair 990. The NIMBUS ground track was parallel to the line between Bravo and Echo. Similar flight track maps were made for all flights.

Both aircraft recorded data at more than one altitude in the vicinity of the Discoverer on each of the three days discussed later except that the NASA aircraft did not fly on July 13. Figure 2 indicates the type of haze size distributions encountered during July. The bulk of the particulates fall in the size range less than 0.3 microns diameter. Therefore, size distribution curves in figure 2 are for the largest particles measured. The shape of the curve for both the low altitudes and the high altitude concentrations are similar. There is a tendency for the size distribution of particles at low altitude to show a lower percentage of particles above 0.5 microns than the higher altitude distributions. The amplitude difference is due to a higher concentration of particles at the lower altitude rather than a difference in the relative amount of particles in a given size range. A very small percentage of the atmospheric particulates encountered had diameters greater than 2.0 microns.

In general, particle concentrations measured by the Condensation Nuclei Counter follow the same pattern in a profile as the concentrations measured by the Bausch and Lomb Dust Counter. Figures 3, 5, and 7 are counts only of particles with diameters as large or larger than 0.3 microns since the Condensation Nuclei Counter was not in operation on those flights.

Following completion of the BOMEX field program, the data recorded on magnetic tape were reduced to values of particle counts per volume and equivalent sea

surface temperatures. The radiosonde and aircraft temperatures and water vapor data along with climatic ozone data were fed into a mathematical model and the theoretical equivalent sea surface temperature at various altitudes through the atmosphere were calculated.

3. COMPUTER SIMULATION

For this study the authors used a radiation transfer model RADIANV developed by Cox and Kuhn at the University of Wisconsin for evaluating the effects of water vapor, ozone, and carbon dioxide on the transfer of infrared radiation. The program has been modified to include hydrometeors and other particulates.

For the purposes of this study, it was required that the program calculate outgoing radiation flux. However, the program RADIANV can determine both outgoing and incoming radiation in the infrared region of the electromagnetic spectrum. The following discussion includes the operation of the program, the input data which must be supplied by the user, and the output of the model.

Three of the features of RADIANV that make it desirable for radiation flux computations are as follows:

a. Transmission coefficients are selected from Smith or Elsasser tables which are included in the program. These tables are frequently updated to give the most accurate values of atmospheric transmissivity.

b. The bandpasses of interest are separated into 10 wavenumber intervals. All computations are accomplished for each 10 wavenumber interval. This gives relatively fine spectral structure to the flux calculations.

c. Either atmospheric aerosols or clouds can be included in the model by entering the scattering, absorption, and extinction volume cross sections for the desired type of cloud or aerosol.

These three facets of the program aid in obtaining spectral detail, accuracy of computation, and realistic modeling of radiation flux divergence through the atmosphere.

Both radiance and irradiance values are computed for each 10 wavenumber interval and each atmospheric layer. A weighting function ($d\tau/d \ln P$) is also part of the output, as well as functions related to the optical depth of each constituent. The program is extremely flexible. It can be used to simulate any infrared remote sensing instrument from radiometer to thermal line scanner by the choice of look angle limits, wavelength interval, and filter functions.

In order to evaluate atmospheric particulates, it was necessary to compute the volume cross sections for scattering, extinction, and absorption for the desired aerosol or cloud model. A separate computer program has been developed from the series of works by Deirmendjian (1959, 1960, 1964, 1969) and Deirmendjian and Clasen (1962). The user of this program must supply indices of refraction for the particulate material for the wavelength range of interest. He also must provide the particle size distribution for the aerosol or cloud model chosen. The output of the program is a punched data deck and a printout of the volume cross sections for scattering, absorption and extinction for each 10 wavenumbers throughout the portion of the infrared spectrum of interest to the user. The data deck then can be inserted into RADIANV for inclusion in the transfer equations.

4. COMPARISON OF COMPUTED AND OBSERVED VALUES OF EQUIVALENT BLACKBODY TEMPERATURE

The following discussion includes a comparison of calculated and measured 8-14 micron and 10-11 micron radiation for three different synoptic situations of interest: cloudless and haze-free, cloudy and hazy, and cloudless and very hazy. The bandpass of the PRT-5 radiometer is 8-14 microns while the bandpass of the NIMBUS MRIR channel 2 is 10-11 microns. The three days representative of these conditions were chosen by participants at the BOMEX Radiation and Particulates Conference of October, 1970. These dates are July 13 (cloudless and haze-free), July 18 (cloudy and hazy), and July 23 (cloudless and very hazy).

On July 13, 1969, the Colorado State University Aero Commander flew a dual mission with the NCAR aircraft participating in BOMEX. The NASA Convair 990 did not fly on this date and consequently only aerosol data for low altitudes up to 9,000 feet msl are available. These data are given in figure 3. The location of the profile was approximately 100 nautical miles WSW of the Discoverer. The profile took place during the period 1440Z to 1451Z. Of particular interest is the very low concentration of particulate material on this occasion. July 13 had a cumulative number of large particles of approximately 10^9 per cubic foot of air at 9,000 feet in comparison to the flights of July 18 and July 23 with 4 and 5 times more, respectively, at the same altitude, as shown in figures 3, 5, and 7.

Figure 4 is a graph of equivalent blackbody temperature versus altitude. The observed values are of sea surface temperature as measured by the Barnes PRT-5 radiometer in the Aero Commander for the lower altitudes and from the NIMBUS MRIR channel 2 for the highest altitude. The calculated values have been determined by the computer model RADIANV, described earlier in section 3. The calculated values are sea surface temperatures which, theoretically, would have been measured if no aerosols were present between the surface and the radiometer. The data utilized by the model included aircraft and radiosonde measurements of air temperature and humidity. Radiosonde data from the nearest ship were used in the program RADIANV when aircraft data were not available. On July 13 the radiosonde data were taken at 1500Z from the USC & GSS Discoverer which was located 13°N, 55°W (figure 1), approximately 100 miles from the actual profile location. Climatic data were used for the ozone mixing ratio input into the model, and for the top of the atmosphere values of temperature and water vapor mixing ratio.

As seen by figure 4, there is very good agreement between the calculated and the observed values of equivalent blackbody temperature. This shows that with very small concentrations of aerosols, such as were observed on July 13, RADIANV accounts accurately for the attenuation of infrared radiation by the molecular constituents in the atmosphere when accurate measurements of those parameters are input into the model.

Figure 5 is of the particle concentrations for the hazy and cloudy case of July 18. Particle concentrations for this day have much higher values than on July 13. The highest values are near the tops of the clouds, which in this case were approximately 8,000 feet msl. Above the clouds particulate concentrations decrease rapidly to near zero as indicated by both Aero Commander and Convair 990 measurements. This profile was flown by both aircraft within 80 nautical miles of the Discoverer. The 1500Z radiosonde data are again used.

Figure 6 shows that the calculated values of blackbody temperature for the July 18 profile, neglecting aerosol and cloud effect, are higher than the observed values. The difference between the observed and the calculated values increases as the altitude increases, indicating that attenuation by atmospheric aerosols (and clouds) must be accounted for in any procedure to determine exact equivalent surface temperatures. For this case no attempt was made to differentiate between

cloud and aerosol effects. Cumulative aerosol amounts were less on July 18 than on July 23 as can be seen by comparing figure 5 to figure 7. Cloud cover on July 18 during the studied time was in several layers: scattered cumulus between 2,000 feet and 3,000 feet; scattered cumulus congestus between 2,000 and 6,000 feet; scattered alto-cumulus near 5,000 feet; and high thin cirrus above 30,000 feet. The difference between observed and calculated temperature values by the NIMBUS MRIR dramatically portray the effect which clouds, especially cirrus, have on the transfer of infrared radiation. The observed value is 19.2°C, whereas the calculated value neglecting the clouds and aerosols is 23.8°C.

Figures 7 and 8 depict the case of July 23--a very hazy day, indeed. The aerosol concentrations were higher than the previous cases and the aerosol concentrations extended to higher altitudes. Thus, the cumulative number of aerosol particles was greater than on the two previous days studied, figures 3 and 5. Cloud effect on July 23 was negligible. The dense haze, identified by BOMEX participants as African dust (Harmattan haze), originated in the desert of western Africa and was carried out over the Atlantic in deep layers. The dust and its associated atmospheric conditions inhibited clouds to a very large degree.

Even so, figure 8 indicates that the difference between observed and calculated temperatures is as great as on July 18 at the aircraft altitudes. The attenuation causing the lower observed temperatures is strictly attenuation by atmospheric aerosols. The NIMBUS MRIR 10-11 micron observation is not as low as on July 18, figure 6, again indicating the disturbing effect of cirrus clouds on radiometric observations from satellite. The data used for July 23 were taken near the Discoverer with both aircraft again within 80 miles of the ship. As before, the 1500Z Discoverer radiosonde data were used.

5. RESULTS AND CONCLUSIONS

The calculated equivalent sea surface temperatures discussed above reflect only the atmospheric constituent attenuation. Knowing that a very light concentration of atmospheric particulates existed on July 13, the closeness of the calculated values to the observed values for that day proves the accuracy of the RADIANV computer simulation for infrared radiation transfer. In this case (figure 4) where the actual sea surface temperature was 27.8°C, the attenuation of infrared energy by the atmosphere gave an observed equivalent temperature at 5,000 feet msl of 24.6°C by the PRT-5 radiometer--a drop of 3.2° from the surface value. The calculated value at 5,000 feet is 24.8°C--a drop of 3.0°. Therefore, the calculated value indicates within 7% the actual attenuation of infrared energy for those atmospheric conditions. This does not take into account the fact that a small concentration of aerosols was present. The calculated value for the NIMBUS MRIR 10-11 micron channel indicates that the total attenuation of infrared energy from the sea surface to the top of the atmosphere gives a brightness temperature decrease of 4.2°C--within 0.3° or 6.7% of the observed drop of 4.5°C.

In contrast to the closeness between calculated and observed values for the haze-free case, July 13, the very haze case, July 23, figure 8, shows the extent to which particulate matter in the atmosphere can attenuate infrared energy. For the 8-14 micron bandpass (PRT-5 radiometer) the observed drop in equivalent temperature was 6.1°C from the sea surface temperature of 28.2° to 22.1°C. The value calculated by RADIANV for decrease in brightness temperature by atmospheric constituents alone was 5.0°C. The 1.1°C difference between the calculated and observed decreases in brightness temperature amounts to 18% of the total observed decrease. This amount of infrared energy, therefore, was attenuated by atmospheric particulates. Even in the case of the 10-11 micron bandpass, it is seen (figure 8) that an extra 1.9°C decrease in brightness temperature occurred over and above the calculated decrease of 5.2°C. The BOMEX study has shown conclusively that the amount of infrared energy attenuated by atmospheric particulate matter is significant. Atmospheric haze cannot be ignored as an attenuating medium when correcting infrared remote sensing measurements from aircraft and satellites.

The effect of particulates can be seen, Table 1, by comparing the refractive indices of pure quartz, a material included in atmospheric dust (Peterson, 1968) to that of liquid water, a known absorber in the infrared (Kondrat'yev, 1969), and by comparing the volume cross sections for the two materials when the same size distribution of particles is used for both, Table II. Although the refractive indices of water and quartz are not similar point for point, the average value over a bandpass of 8-14 microns is similar for both. Likewise, and even more striking, is the fact that over a wide bandpass the average of the volume cross sections for quartz are larger than the average for liquid water. This means that the attenuation by a quartz aerosol is greater than for water when the size distribution of the particles is the same for both materials.

6. REFERENCES

Davies, C.N. (1966). Aerosol Science, Academic Press, Inc., New York, 468pp.

Deirmendjian, D. (1959). "The Role of Water Particles in the Atmospheric Transmission of Infrared Radiation," Quarterly Journal of the Royal Meteorological Society, 85, 404.

_____ (1960). Atmospheric Extinction of Infrared Radiation, The Rand Corp., Paper P-1880, 11pp.

_____ (1964). "Scattering and Polarization Properties of Water Clouds and Hazes in the Visible and Infrared," Applied Optics, 3, 187.

_____ (1969). Electromagnetic Scattering on Spherical Polydispersions, American Elsevier Publishing Co., Inc., New York, 290pp.

_____, and R.J. Clasen (1962). Light Scattering on Partially Absorbing Homogeneous Spheres of Finite Size, The Rand Corporation, Paper R-393-PR, 44pp.

Goody, R.M. (1964). Atmospheric Radiation, Oxford University Press, London, 436pp.

Junge, C.E. (1963). Air Chemistry and Radioactivity, Academic Press, Inc., New York, 382pp.

Kondrat'yev, K. Ya. (1969). Radiation in the Atmosphere, Academic Press, Inc. New York, 912pp.

Marlatt, W.E. (1964, 1965). Investigation of the Temperatures and Spectral Emissivity Characteristics of Cloud Tops and of the Earth's Surface, Colorado State University Atmospheric Science Dept., Tech. Paper No. 51, 13pp. and Tech. Paper No. 72, 26pp.

_____ (1965). The Measurement of the Surface Temperature of the Earth, Colorado State University Atmospheric Science Dept., Tech. Paper No. 64, 11pp.

Peterson, J.T. (1968). Measurement of Atmospheric Aerosols and Infrared Radiation Over Northwest India and Their Relationship, Tech. Report No. 38, University of Wisconsin, 165pp.

Reeser, W.K. (1969). Haze Distributions in the Troposphere, Colorado State University Atmospheric Science Tech. Paper No. 139, 106pp.

Wolfe, W.L., ed. (1965). Handbook of Military and Infrared Technology, U.S. Government Printing Office, Washington, 906pp.

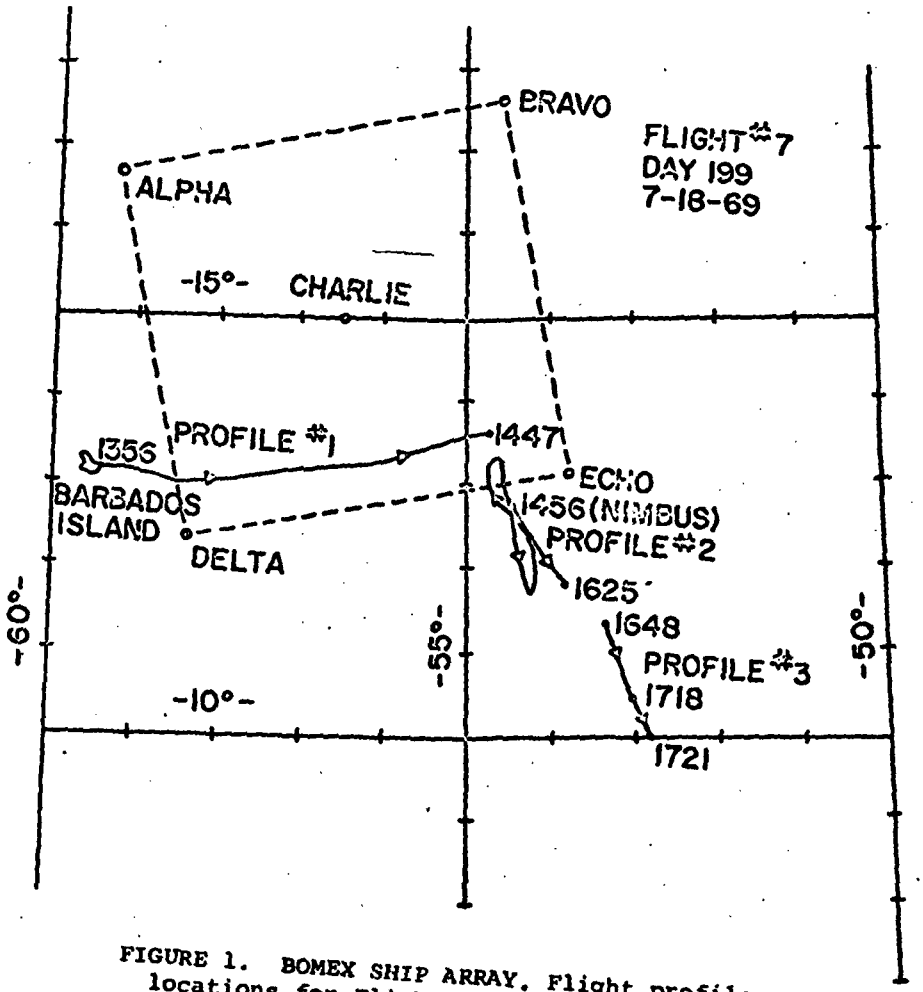

FIGURE 1. BOMEX SHIP ARRAY. Flight profile locations for Flight #7, July 18, 1969 are shown.

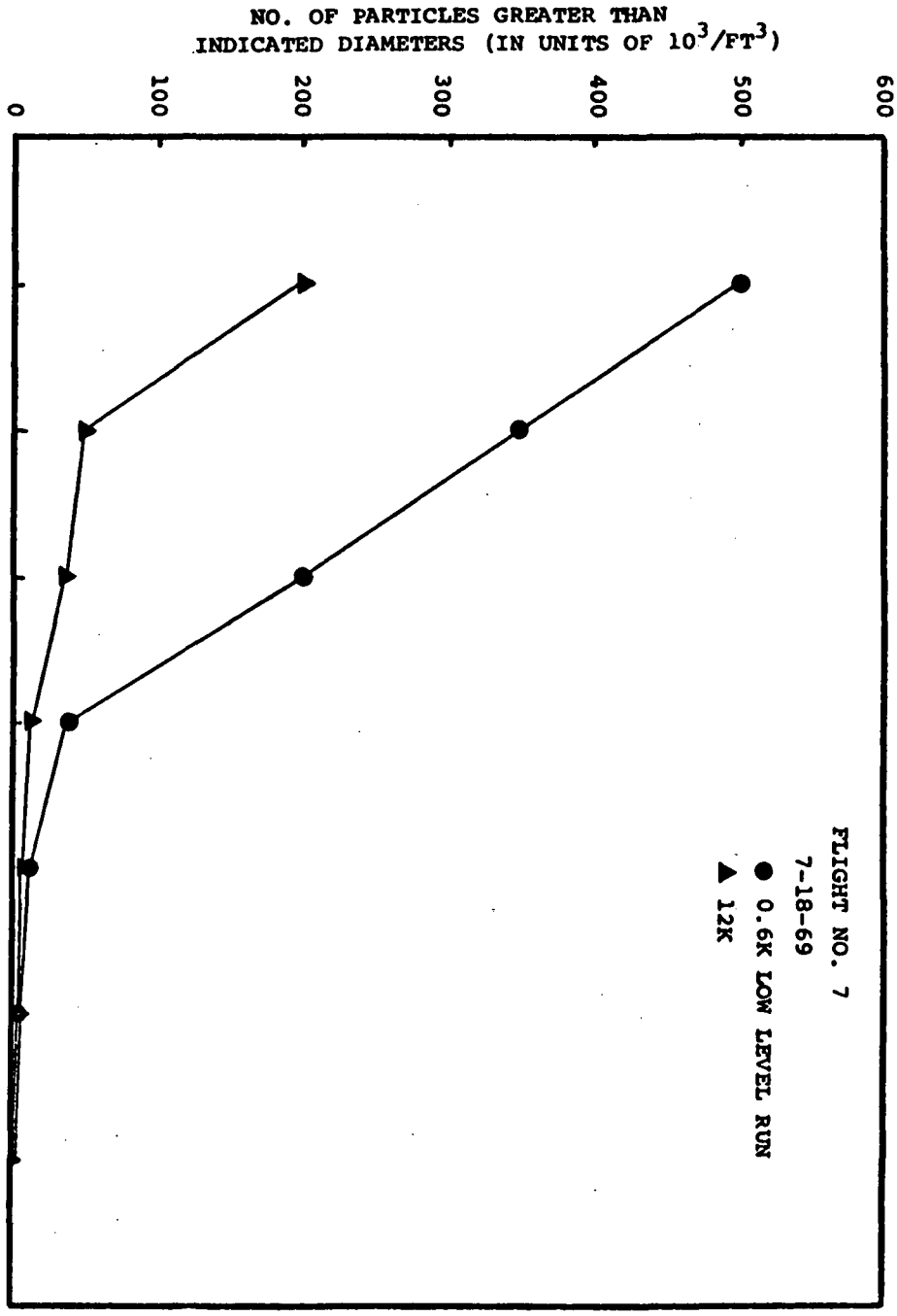

FIGURE 2. TYPICAL SIZE DISTRIBUTIONS OF LARGE ATMOSPHERIC PARTICULATES.

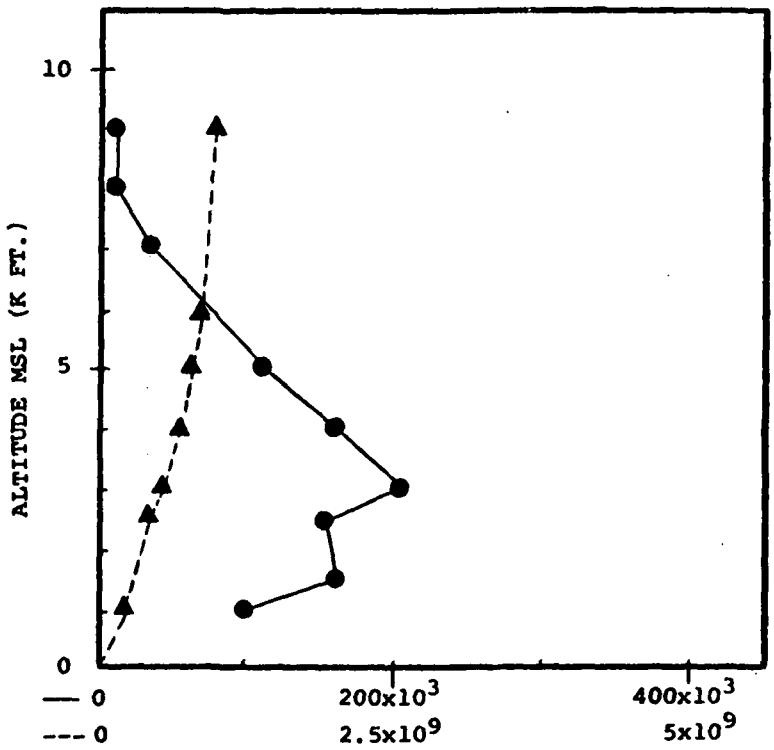

— No. particles with dia. greater than .3 micron at each altitude (per ft^3)
--- Cumulative no. particles with dia. greater than .3 micron

FIGURE 3. JULY 13, 1969, AEROSOL CONCENTRATION PROFILE. K ft. means thousands of feet.

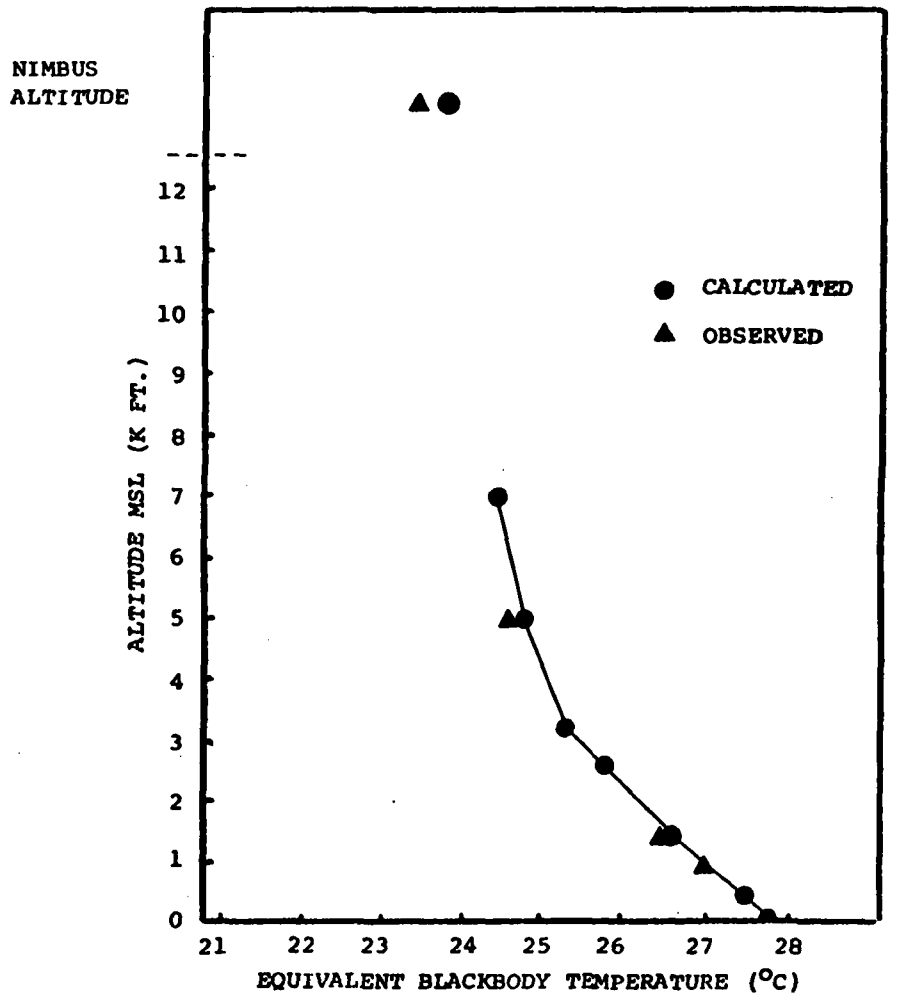

FIGURE 4. COMPARISON OF OBSERVED AND CALCULATED SEA SURFACE TEMPERATURES FOR JULY 13, 1969.

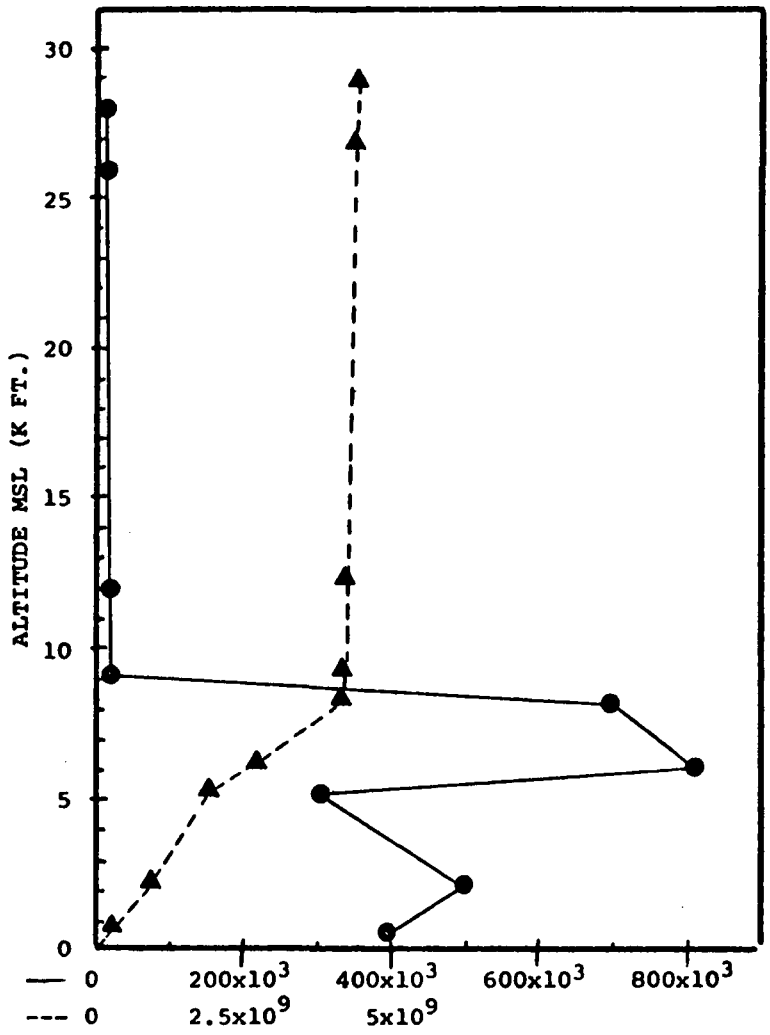

— No. particles with dia. greater than .3 micron at each altitude

--- Cumulative no. particles with dia. greater than .3 micron

FIGURE 5. JULY 18, 1969, AEROSOL CONCENTRATION PROFILE.

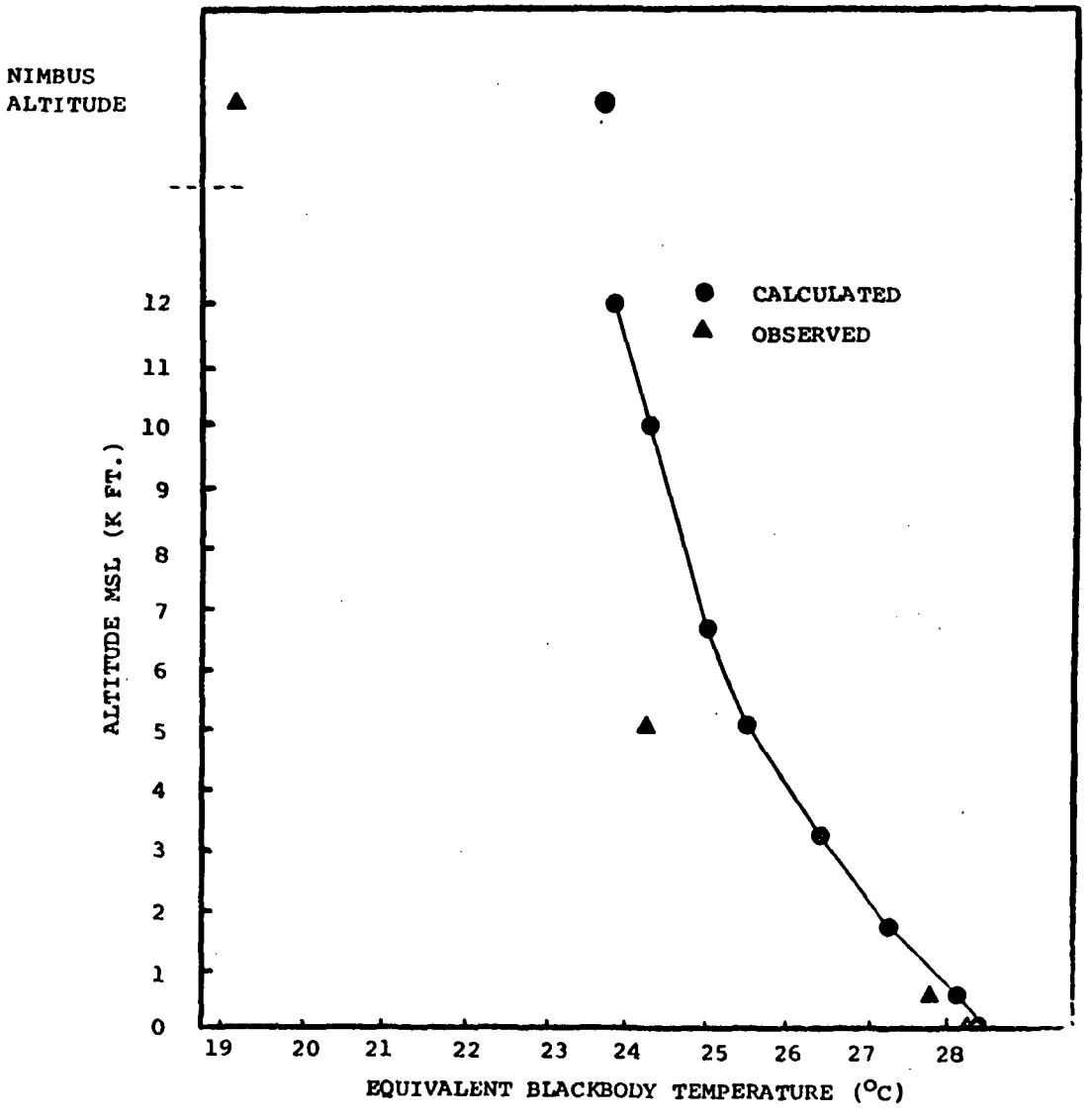

FIGURE 6. COMPARISON OF OBSERVED AND CALCULATED SEA SURFACE TEMPERATURES FOR JULY 18, 1969.

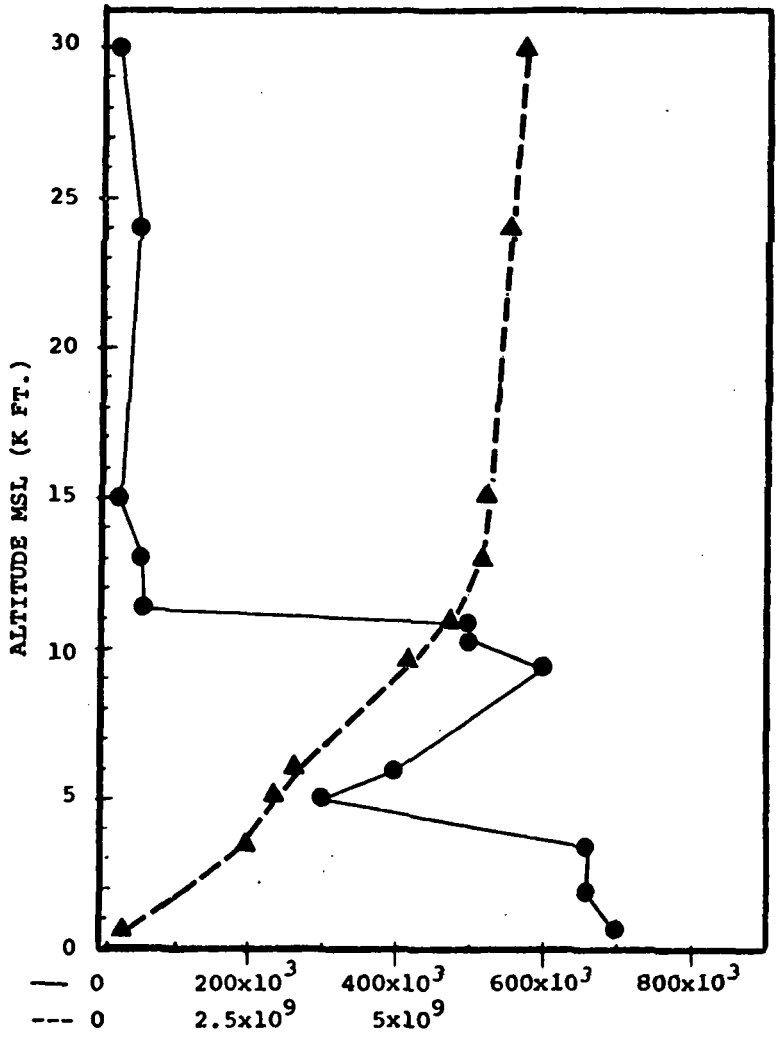

— No. particles with dia. greater than .3 micron at each altitude

--- Cumulative no. particles with dia. greater than .3 micron

FIGURE 7. JULY 23, 1969, AEROSOL CONCENTRATION PROFILE.

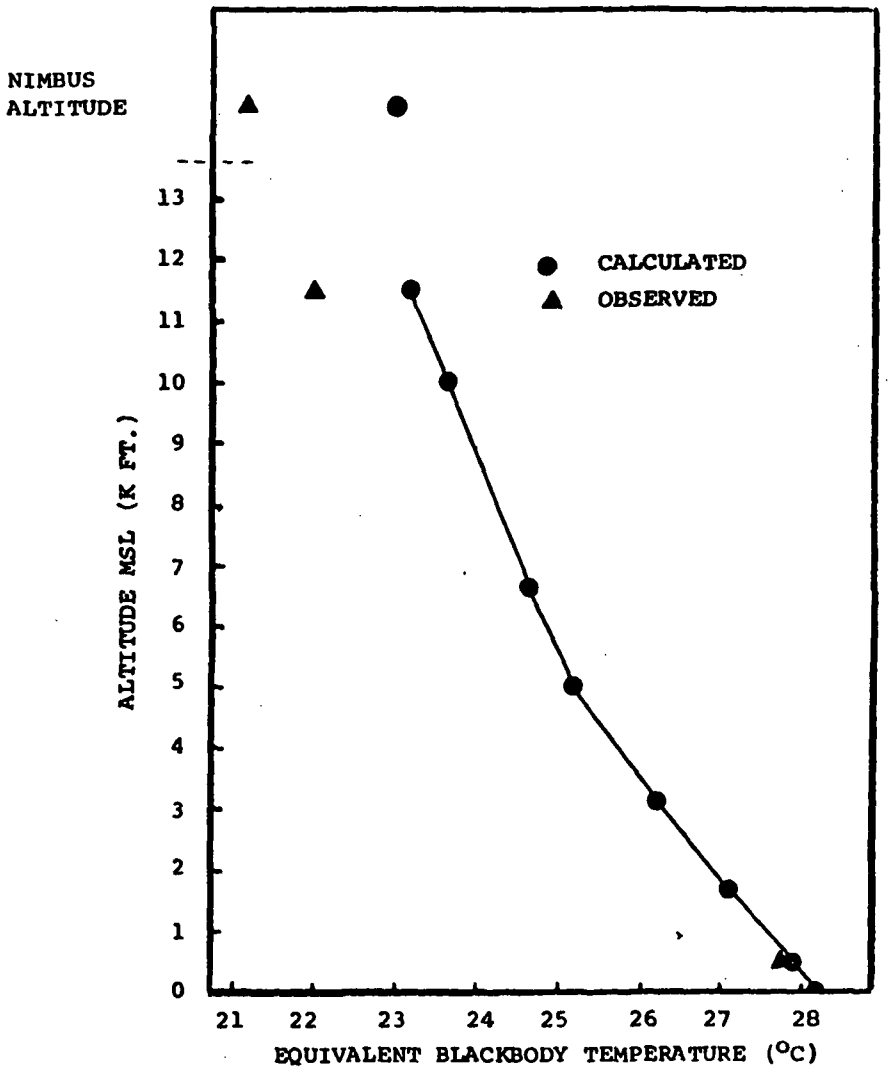

FIGURE 8. COMPARISON OF OBSERVED AND CALCULATED SEA SURFACE TEMPERATURES FOR JULY 23, 1969.

TABLE I. REFRACTIVE INDICES OF QUARTZ AND LIQUID WATER. (M = REAL - i IMAGINARY).

	REFRACTIVE INDICES OF QUARTZ		REFRACTIVE INDICES OF LIQUID WATER	
$\lambda(\mu)$	REAL	IMAGINARY	REAL	IMAGINARY
15.0	---	---	1.330	.430
14.5	1.770	.078	---	---
14.0	---	---	1.275	.358
13.5	1.970	.050	1.245	.320
12.5	1.830	.487	1.190	.244
11.5	.800	.023	1.145	.153
10.5	.267	.028	1.185	.069
9.5	3.000	1.600	1.245	.044
8.5	.167	1.643	1.286	.038
7.5	.800	.049	1.303	.035
AVERAGE	1.325	.495	1.237	.163

TABLE II. VOLUME CROSS SECTIONS FOR EXTINCTION, ABSORPTION, AND SCATTERING IN UNITS OF KM^{-1} FOR QUARTZ AND LIQUID WATER. Size distribution of both materials is given by $n(R) = (1.32 \times 10^{8})$ R exp $[-(200)(R)^{2}]$.

	VOLUME CROSS SECTIONS FOR QUARTZ			VOLUME CROSS SECTIONS FOR LIQUID WATER		
$\lambda(\mu)$	EXTINCTION	ABSORPTION	SCATTERING	EXTINCTION	ABSORPTION	SCATTERING
15.0	----	----	----	$.193 \times 10^{-10}$	$.193 \times 10^{-10}$	$.445 \times 10^{-24}$
14.5	$.128 \times 10^{-13}$	$.128 \times 10^{-13}$	$.777 \times 10^{-24}$	----	----	----
14.0	----	----	----	$.172 \times 10^{-10}$	$.172 \times 10^{-10}$	$.403 \times 10^{-24}$
13.5	$.138 \times 10^{-11}$	$.138 \times 10^{-11}$	$.134 \times 10^{-23}$	$.189 \times 10^{-10}$	$.189 \times 10^{-10}$	$.437 \times 10^{-24}$
12.5	$.149 \times 10^{-10}$	$.149 \times 10^{-10}$	$.182 \times 10^{-23}$	$.885 \times 10^{-11}$	$.885 \times 10^{-11}$	$.233 \times 10^{-24}$
11.5	$.322 \times 10^{-11}$	$.322 \times 10^{-11}$	$.173 \times 10^{-24}$	$.104 \times 10^{-10}$	$.104 \times 10^{-10}$	$.194 \times 10^{-24}$
10.5	$.101 \times 10^{-9}$	$.101 \times 10^{-9}$	$.253 \times 10^{-22}$	$.101 \times 10^{-11}$	$.101 \times 10^{-11}$	$.178 \times 10^{-24}$
9.5	$.146 \times 10^{-10}$	$.146 \times 10^{-10}$	$.119 \times 10^{-22}$	$.215 \times 10^{-11}$	$.215 \times 10^{-11}$	$.396 \times 10^{-24}$
8.5	$.184 \times 10^{-9}$	$.184 \times 10^{-9}$	$.412 \times 10^{-21}$	$.146 \times 10^{-11}$	$.146 \times 10^{-11}$	$.726 \times 10^{-24}$
7.5	$.953 \times 10^{-12}$	$.953 \times 10^{-12}$	$.649 \times 10^{-24}$	$.191 \times 10^{-11}$	$.191 \times 10^{-11}$	$.118 \times 10^{-23}$
AVERAGE	$.386 \times 10^{-10}$	$.386 \times 10^{-10}$		$.0903 \times 10^{-10}$	$.0903 \times 10^{-10}$	

Appendix III.

APPENDIX III. COMPUTED AND CALCULATED INFRARED TRANSFER THROUGH CLEAR AND CLOUDY ATMOSPHERES.

On May 9, 1967, the NASA CV990 and the Colorado State University aircraft made a number of profiles off the coast of California, flying below clouds, through clouds, and above clouds. Dr. Peter Kuhn's upward-looking Barnes PRT-5 radiometer (aboard the CV990) was filtered from 765 to 1385 cm^{-1} and recorded the following results.

When off to the side of the clouds, the data were as follows:

Pressure	Radiance (watts cm^{-2} ster.$^{-1}$)
875 mb.	14.95
729 mb.	10.49
590 mb.	6.41

The program RADIANV was run using the data from the nearest radiosonde station with the following results for the CLEAR SKY case:

Pressure	Radiance (watts cm^{-2} ster.$^{-1}$)
875 mb.	27.76
729 mb.	18.38
590 mb.	9.76

Dr. Kuhn's radiometer data for the CLOUDY condition with the bottom of the cloud at 875 mb. and the top at 590 mb. were as follows:

Pressure	Radiance (watts cm^{-2} ster.$^{-1}$)
875 mb.	36.96
782 mb.	36.34

No value was available at 590 mb.

RADIANV was run using as cloud volume cross section data an EXTCOEF calculation based on drop size distribution and number concentration of drops measured by the CSU aircraft cloud drop sampler system. The data from RADIANV with the cloud information were as follows:

Pressure	Radiance (watts cm^{-2} $ster.^{-1}$)
875 mb.	24.18
782 mb.	22.60
590 mb.	11.81

The discrepancies in the "no cloud" case are large, but the trend between levels in both the observed and the calculated situations is the same showing a loss of approximately one-third of the received energy between each of the chosen levels. However, the results of the cloudy case are very dissimilar between the observed and the calculated situations. Dr. Kuhn's data show a much larger value of radiance below and in the cloud than in the clear sky case, while RADIANV indicates slightly less radiance below the cloud and slightly more radiance in and at the top of the cloud than does the clear sky case. The loss between layers for the calculated case is in the correct direction but larger than observed.

The reason for the large difference between observed, calculated, and the incorrect calculation of a smaller radiance below the cloud than the clear sky case is probably due to the fact that only forward scattering and extinction are calculated by EXTCOEF for the cloud droplets while they actually have angular

components which may need to be included. A second reason for the discrepancies is that no contribution from the earth's surface to the radiational energy balance of the cloud is included. These factors may be added in the near future.

COLLEGE OF FORESTRY AND NATURAL RESOURCES

THE DEPARTMENT OF WATERSHED SCIENCE

was formulated in 1970 to provide a framework for the undergraduate, graduate, and research investigation of the principles of watershed management, bioclimatology, and remote sensing of natural resources.

COLORADO STATE UNIVERSITY

FORT COLLINS, COLORADO